Hindawi
Cellular Microbiology
Volume 2022, Article ID 4017442, 32 pages
https://doi.org/10.1155/2022/4017442

Research Article

Study on Analysis of Several Molecular Identification Methods for Ciliates of Colpodea (Protista, Ciliophora)

Yumeng Song,[1] **Tingting Hao**,[1] **Bailin Li**,[1] **Weibin Zheng**,[1] **Lihui Liu**,[1] **Li Wang**,[1] **Ying Chen**,[2] **and Xuming Pan**[1]

[1]*Key Laboratory of Biodiversity of Aquatic Organisms, Harbin Normal University, Harbin 150025, China*
[2]*School of Civil and Environmental Engineering, Harbin Institute of Technology (Shenzhen), Shenzhen 518055, China*

Correspondence should be addressed to Ying Chen; chenying@hit.edu.cn and Xuming Pan; pppppp206@126.com

Received 7 March 2022; Revised 30 April 2022; Accepted 24 May 2022; Published 28 June 2022

Academic Editor: Jayaprakash Kolla

The application of molecular techniques to accurately identify protozoan species can correct previous misidentifications based on traditional morphological identification. Colpodea ciliates have many toxicological and cytological applications, but their subtle morphological differences and small body size hinder species delineation. Herein, we used *Cox I* and *β-tubulin* genes, alongside fluorescence in situ hybridization (FISH), to evaluate each method in delineating Colpodea species. For this analysis, *Colpoda harbinensis* n. sp., *C. reniformis*, two populations of *C. inflata*, *Colpoda* compare *grandis*, and five populations of *Paracolpoda steinii*, from the soil in northeastern China, were used. We determined that (1) the *Cox I* gene was more suitable than the *β-tubulin* gene as a molecular marker for defining intra- and interspecific level relationships of *Colpoda*. (2) FISH probes designed for *Colpoda* sp., *C. inflata*, *Colpoda* compare *grandis*, and *Paracolpoda steinii*, provided rapid interspecific differentiation of Colpodea species. (3) *Colpoda harbinensis* n. sp. was established and mainly characterized by its size in vivo (approximately $80 \times 60\,\mu$m), a reniform body in outline, one macronucleus, its spherical shape, a sometimes nonexistent micronucleus, 11–15 somatic kineties, and five or six postoral kineties. In conclusion, combining oligonucleotide probes, DNA barcoding, and morphology for the first time, we have greatly improved the delineation of Colpodea and confirmed that *Cox I* gene was a promising DNA barcoding marker for species of Colpodea, and FISH could provide useful morphological information as complementing traditional techniques such as silver carbonate.

1. Introduction

The increasing diversity of ciliates requires multiple methodological tools for their correct identification [1–8]. However, given the constraints of professional or industrial practices, achieving accurate and rapid identification can be challenging via a single method. In the past, Ciliophora identification relied mainly on either morphological and ultrastructural features or small subunit (SSU) ribosomal (r) DNA sequence analysis [9–16]. Although morphological analysis is a valuable technique for identifying ciliates, it can be time-consuming and laborious [17], while SSU rDNA sequence analysis has limitations in distinguishing between closely related species.

Several surveys of DNA barcoding in Ciliophora have shown a high prevalence [18–22]. The *Cox I* gene is a suitable marker for resolving the interspecific and intraspecific relationships of *Paramecium* spp. [22]. The internal transcribed spacer 2 region (ITS2) is also a strong barcoding candidate for identifying the closely related Tintinnids [23]. Molecular phylogenies and genetic measurements based on variable regions of nuclear genes demonstrated that the ITS2 and LSU-D1/D2 regions are more suitable for delineating *Euplotes* [24]. Fluorescent probes targeting small subunit ribosomal RNA (SSU-r RNA) have been designed and optimized for fluorescence in situ hybridization (FISH), resulting in the accurate and rapid identification of pathogenic ciliates (e.g., *Pseudocohnilembus persalinus*, *Boveria labialis*, and *B. subcylindrica*) [25–28]. FISH allows for molecular identification of targeted organisms in mixed populations, overcoming the negatives of morphological methods and producing timely detection results. However, there are

currently no available fluorochrome-labeled oligonucleotide probes for the genus *Colpoda*.

The class Colpodea (Small and Lynn [29]) comprises approximately 60 genera and 200 species, with most living in terrestrial and semiterrestrial habitats, such as mosses, leaf litter, soil, and tree holes [30–34]. However, this is likely only a subset of the total diversity, with a high number of species likely undiscovered [35]. Colpodea is typically characterized by high technical requirements for staining, environmental sensitivity, susceptibility to dormant cysts, and few multigene sequences, resulting in long-standing problems with species identification and taxon attribution [13, 30, 36–41]. To date, the identification of ciliates of Colpodea has relied solely upon morphological features and SSU rDNA sequence analysis. However, with the conservative evolution of SSU rDNA alongside various issues such as asynchronous evolution with morphology, delineation remains problematic. Therefore, other methods, including DNA barcoding and oligonucleotide probes, should be developed to accurately and rapidly identify Colpodea. The uses of DNA barcoding and FISH are universally applicable tools that can identify ciliates and confirm taxonomic relationships previously based on ultrastructural and other morphological features [22, 26–28, 42].

Nonetheless, there is still no universal gene marker for species discrimination of ciliates. In the present investigation, we assessed the suitability of DNA barcoding and oligonucleotide probe techniques to delineate ten newly isolated Chinese populations of five Colpodea species. Specifically, we investigated the barcoding utility of *β-tubulin* and the mitochondrial *cox1* genes, both at the congeneric and conspecific levels, in order to analyze the reliabilities of molecular identification methods for ciliates of Colpodea.

2. Material and Methods

2.1. Ciliate Isolation, Observation, and Identification. Five species were collected from soil in northeastern China and treated with nonflooded Petri dish cultures as described in Foissner et al. [43]. After isolation, specimens were maintained in Petri dishes in the laboratory for three days. Clonal cultures were then established and maintained at room temperature in boiled water amended with a grain of wheat to enrich natural bacteria as food for the ciliates. Isolated cells were observed and photographed in vivo using differential interference contrast microscopy. The silver carbonate [44] was used to reveal the infraciliature in different morphogenetic stages. Stained specimens were counted and measured at magnifications of ×100–1250, and mapping was performed with the help of a drawing device. Classification and terminology are mainly according to Foissner [30] and Lynn [45].

2.2. DNA Extraction, PCR Amplification, and Sequencing. Five cells from each monoclone were isolated under the stereomicroscope using micropipettes and washed with double distilled water to remove contaminants. Cells were then transferred to an Eppendorf tube with a small amount of water. Total genomic DNA of the cells was extracted with the DNeasy & Tissue Kit (Shanghai, QIAGEN, Germany) according to the manufacturer's instructions.

The *β-tubulin* and the *Cox I* genes were amplified using the polymerase chain reaction (PCR). PCR primers are listed in Table 1, and conditions of the respective PCR reactions are summarized in Table 2. Sequencing was performed Shanghai Sangon Biological Engineering and Technical Service Company (Shanghai, China). 36 new molecular sequences of *β-tubulin* and *Cox I* genes were generated from five species of Colpodea. All the sequences were aligned using Clustal W implemented in BioEdit 7.0.1 [46].

2.3. Cell Fluorescence In Situ Hybridization (FISH). Probes (Table 3) were designed using the probe design tool as implemented in the ARB software package for the SSU-rDNA sequences of the present *Colpoda harbinensis* n. sp, *C. inflata*, *Colpoda* compare *grandis*, and *Paracolpoda steinii*. Generated probes were checked against the GenBank sequence collection by a standard nucleotide-nucleotide BLAST search [47]. FISH was used to visualize Colpodea spp. above both in field samples and a mixture of species as well as *Coleps hirtus* that frequently occurred in the same habitats as the negative control. Cells were fixed with 50% Bouin's solution and filtered onto a 2 μm-pore-size cellulose nitrate membrane (25 mm in diameter) using low under pressure. The membrane was then washed five times with 2 ml of filtered sterile water. The basic hybridization follows the protocol of Stoeck et al. [48] and Zhan et al. [26].

2.4. Phylogenetic Analyses. Phylogenetic trees were inferred using maximum likelihood (ML) and Bayesian inference (BI) methods. ML analyses were constructed by RAxML-HPC2 v8.2.12 [49], and BI analyses were constructed by MrBayes v3.2.7a [50], both on the CIPRES Science Gateway (URL: http://www.phylo.org/sub_sections/portal). The ML and BI trees based on 18S rRNA gene were constructed according to the GTR + I + G model chosen by the MrModeltest v.2.0 program [51]. ML analysis was done using rapid bootstrap with 1,000 nonparametric bootstrap replicates. Bayesian posterior probabilities were calculated by running four chains for 10,000,000 generations, with the cold chain sampling every 10,000 generations. The first 25% of sampled trees were discarded as burn-in. Support values < 75%/0.75 (ML/BI) was considered as low, 75%/0.75–90%/0.90 (ML/BI) as moderate, and >90%/0.90 (ML/BI) as high. MEGA 7.0 [52] was utilized to visualize tree topologies.

2.5. Haplotype Networks. A *β-tubulin* haplotype network was constructed for *Paracolpoda steinii* and *Colpoda inflata*, using the TCS method [53] as implemented in PopART ver. 1.7 [54]. Mutations in *β-tubulin* sequences were displayed as line segments on the haplotype network.

3. Results

3.1. Morphological Description of Chinese Populations of Four Known Colpodea Species

3.1.1. Colpoda reniformis (Figures 1(a) and 1(b)). Specifications are as follows: size 123 – 130 × 85 – 95 μm in vivo, body

Table 1: Primers used for amplification of two molecular markers analyzed in this study.

Molecular marker	Primer name	Primer sequence (in 5′ to 3′ direction)	Reference
Cox I	MOU08–121	TCAGGAGCTGCMTTAGCHACYATG	Whang et al. [68]
	MOU08–122	TARTATAGGATCMCCWCCATAAGC	Whang et al. [68]
β-Tubulin	X–349A	CGTCTATTACAATGAAGCCACT	Present study
	X–349B	ATTCCATCTCGTCCATACCTT	Present study

Table 2: Conditions of PCR reactions used for amplification of three molecular markers analyzed in this study.

Primer name	PCR program			Reference
	Initial denaturation	Cycling (denaturation, annealing, extension)	Final extension	
X–349	94°C/5 min	35 cycles: 94°C/30 s, 51°C/75 s, 72°C/90 s	72°C/10 min	Present study
MOU08	94°C/2 min	30 cycles: 94°C/30 s, 50°C/30 s, 72°C/2 min		Whang et al. [76]

Table 3: 18S rRNA targeted oligonucleotide probes used to test FISH.

Target organism	Probe name	Probe sequence (in 5′ to 3′ direction)
Colpoda grandis	YdaA	AGAAGGTTCACCGGATCACTCA
Colpoda inflata pop. 1	GRA	TTGGTCCGACTTCTCCTTCCTC
Colpoda inflata pop. 2	ZLA	ACTCCCCACAACCAAGTCAAGC
Paracolpoda steinii pop. 4	TSBS	CAGCAATGGGTTTTGTGATGAT
Colpoda harbinensis n. sp.	BBxA	CAGGCTCACTCAAAATCGGTAG

monk's cap nephroid in shape, with left margin slightly curved and the right margin "C"-shaped (Figures 1(a) and 1(b)). Diagonal groove was present (Figure 1(a)). One macronucleus, nearly spherical, is located in the middle of the body, and no micronucleus was observed (Figure 1(b)). Contractile vacuole situated in the posterior 1/3 of the body, approximately 4 μm in diameter during diastole. Extrusomes were conspicuous and numerous, approximately 2 μm (Figure 1(a)): 27–39 somatic kineties, oral located 1/2 of the body, amd 13–15 postoral kineties (Figures 1(a) and 1(b)).

3.1.2. Colpoda Compare grandis (Figures 1(c)–1(e)). Specifications are as follows: cell 190 – 195 × 130 – 140 μm in size, round reniform in outline, laterally flattened, and no postoral sack (Figures 1(c) and 1(d)), brownish cytoplasm usually contained food vacuoles, one macronucleus, roughly spherical, positioned in the middle and anterior part of the cell, no micronucleus (Figure 1(d)), contractile vacuole located posteriorly, and approximately 4 μm in diameter during diastole. No extrusomes were observed. There is a forward swimming in a spiral pattern in the water. Somatic cilia were closely arranged, approximately 10 μm long. Diagonal groove was not observed: left oral polykinetid on vestibular bottom, elongated square (Figure 1(e)): 28–30 somatic kineties and 12–14 postoral kineties.

3.1.3. Two Populations of Colpoda inflata (Figures 1(f)–1(m)). Population 1 had a body size of 63 – 72 × 44 – 50 μm in vivo, while population 2 was slightly larger, with a body size of about 85 – 88 × 65 μm. Other characteristics of the two populations were similar: elongated reniform in outline, with soft, rough cortex, and slightly dark endoplasm (Figures 1(f)–1(k)). Oral is located 1/2 of the body. One macronucleus is roughly spherical or oval, anterior, or posterior to the middle of the body; single micronucleus, either oval or crescent-shaped, is closely adjacent to the macronucleus (Figures 1(h), 1(j), and 1(k)). One contractile positioned at the end of the body (Figures 1(g) and 1(i)). Depending on the refraction, granules of different sizes appeared brownish yellow or black under bright-field light microscopy. Diagonal grooves were absent: 23–25 somatic kineties. Left oral polykinetid on elongate elliptic (Figures 1(l) and 1(m)): seven or eight postoral kineties.

3.1.4. Five Populations of Paracolpoda steinii (Figure 2). Five populations were present in this collection, and all interpopulation variation was within the variable range. Population 1 had a greater range of individual size variation than the other four populations (55.5 – 70.6 × 36.6 – 45.4 μm). Population 3 had a slightly longer body length than population 2, but a similar body width (55 – 65 × 35 – 40 μm vs. 50 – 65 × 35 – 40 μm) (Figures 2(c)–2(h)). Populations 4 and 5 were very similar in body size in vivo (60 – 65 × 40 – 45 μm vs. 65 – 70 × 40 – 45 μm) (Figures 2(i)–2(m)). Other characteristics were almost identical: lateral appearance reniform, preoral portion remarkably short (1/4–1/3 of body length), usually slightly ventrally inclined, flattened slightly to 2: 1, in ventral and dorsal aspect pyriform to moderately broadly wedge-shaped, and distinct diagonal grooves (Figures 2(a), 2(c), 2(f), 2(i), and 2(c)). Macronucleus slightly to distinctly ellipsoid is usually near the center of the cell. Micronucleus calotte-shaped

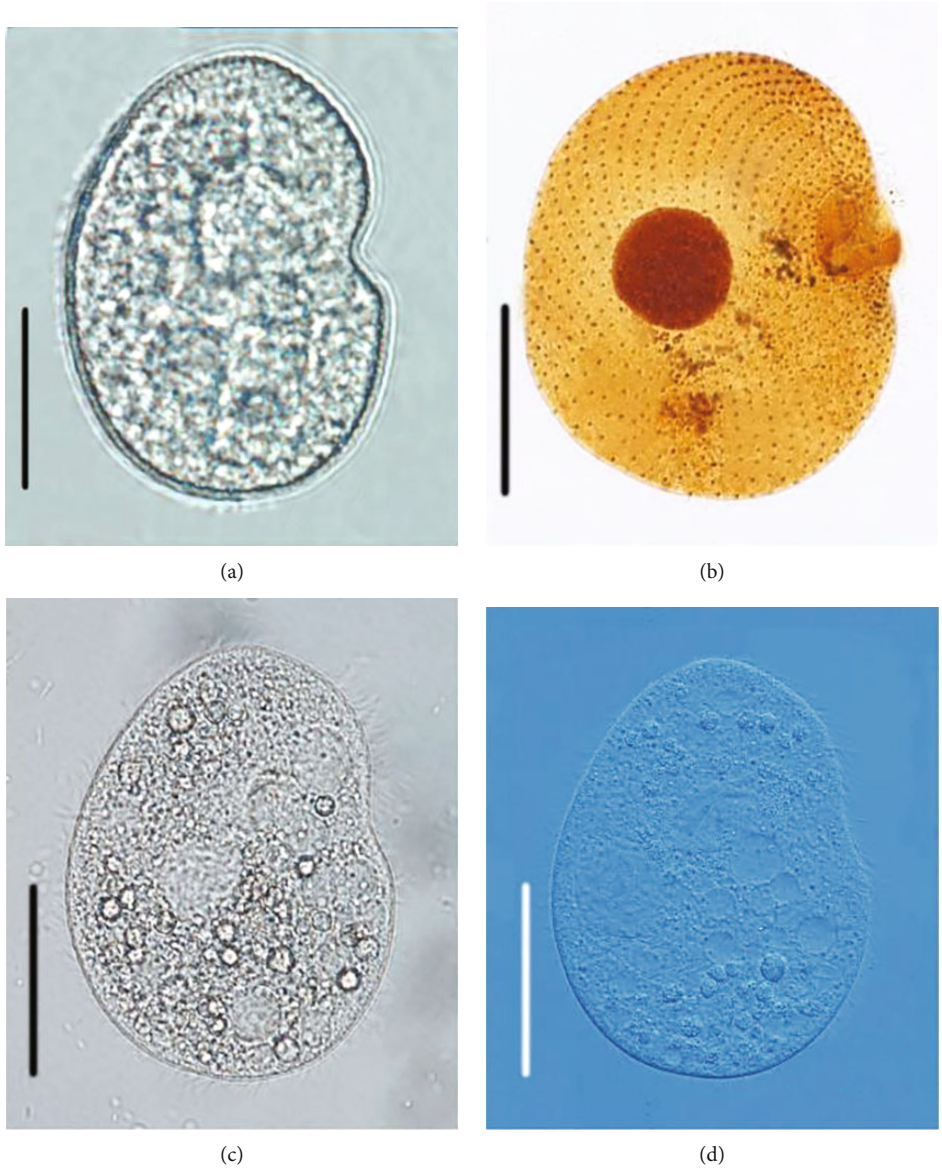

(a) (b)

(c) (d)

Figure 1: Continued.

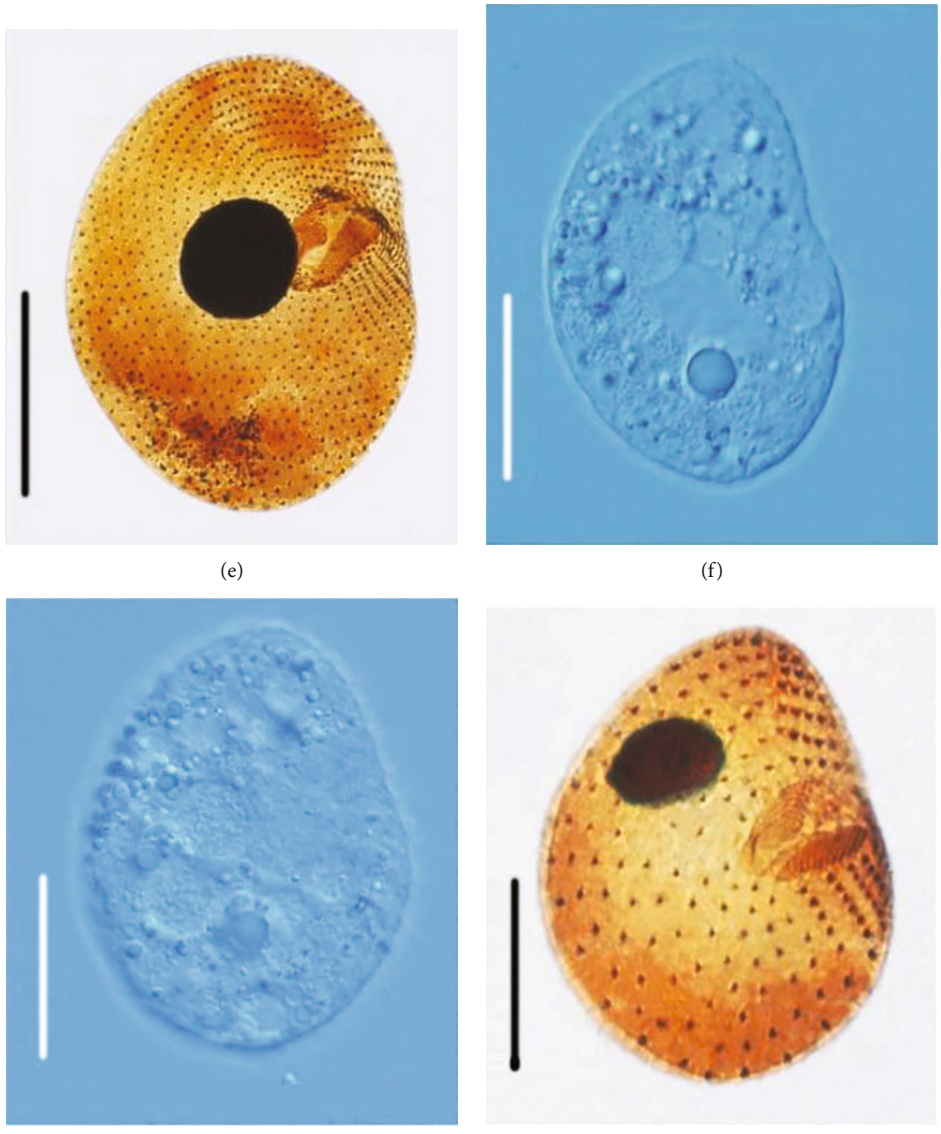

(e) (f)

(g) (h)

Figure 1: Continued.

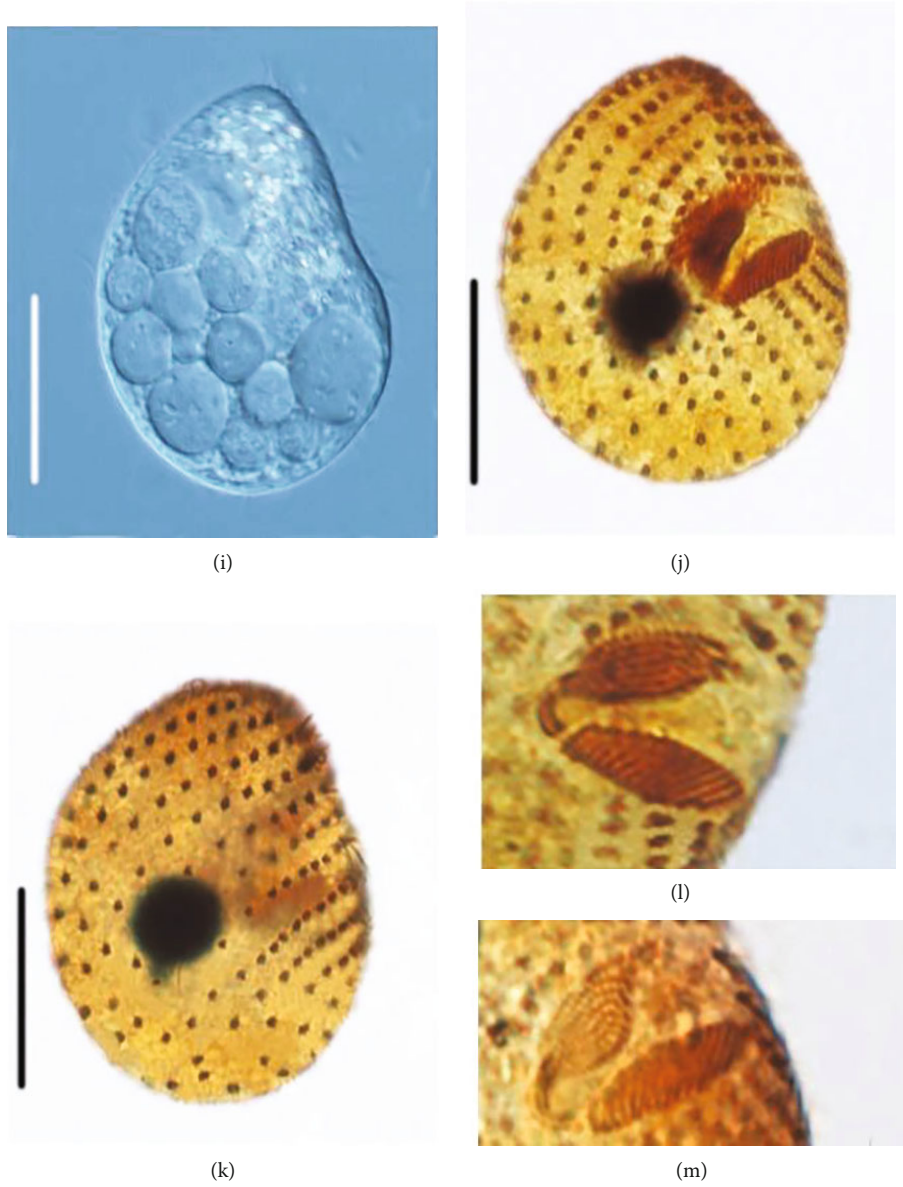

Figure 1: Photomicrographs from life (a, c, d, f, g, i) and after silver carbonate staining (b, e, h, j–m). (a, b) *Colpoda reniformis*, photomicrographs from life (a) and after silver carbonate staining (b). (c)–(e) *Colpoda* compare *grandis*, photomicrographs from life (c, d) and after silver carbonate staining (e); (f–h, m) *Colpoda inflata* population 1, photomicrographs from life (f, g) and after silver carbonate staining (h), dorsal views to demonstrate the oral (m); (i–k, l) *Colpoda inflata* population 2, photomicrographs from life (i) and after silver carbonate staining (j, k), dorsal views to demonstrate the oral (l). Scale bars = 60 μm (a, b); 90 μm (c)–(e); 40 μm (f)–(k).

was attached to macronucleus (Figures 2(b), 2(d), 2(e), 2(g), 2(h), 2(j), 2(l), and 2(m)). Contractile vacuole was located at the posterior end, approximately 3 μm long, during diastole with small collecting vesicles and a single excretory pore in the center of the posterior pole. Oral apparatus in anterior third. Oral polykinetids were protrude. Left polykinetids were vertically distributed. Left polykinetids are elliptical, occasionally slightly wedge-shaped or rectangular (Figures 2(n)–2(o)), and moves rapidly, mostly rotating toward the back of the body or marching directly forward. Somatic cilia were approximately 8 μm long: 9–11 somatic kineties.

3.2. Phylogenetic Analyses Based on 18S rRNA Gene Sequence Data. Phylogenetic trees were constructed using ML and BI and produced similar topologies; therefore, only the ML trees and their support values from both methods are shown. According to the 18S-rRNA gene tree, all four orders within Colpodea were monophyletic (Figure 3). Colpodida and Cyrtolophosidida clustered together to form a clade, with Bursariomorphida as a sister clade, while the order Platyophryida occupied the basal position within Colpodea.

The newly sequenced species *Paracolpoda steinii* was sister to the clade clustered by *P. steinii* (KJ607914) and

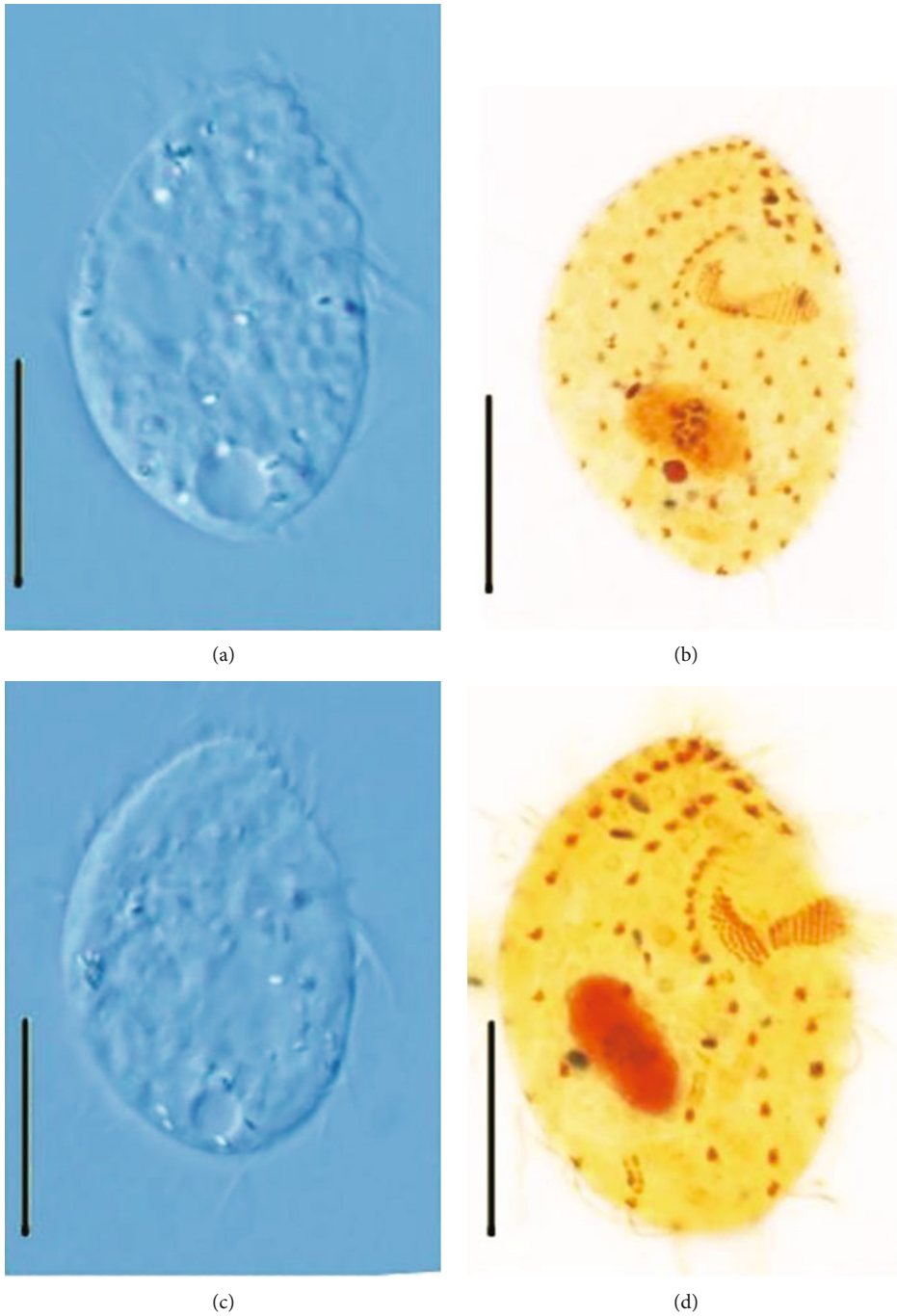

(a) (b)

(c) (d)

Figure 2: Continued.

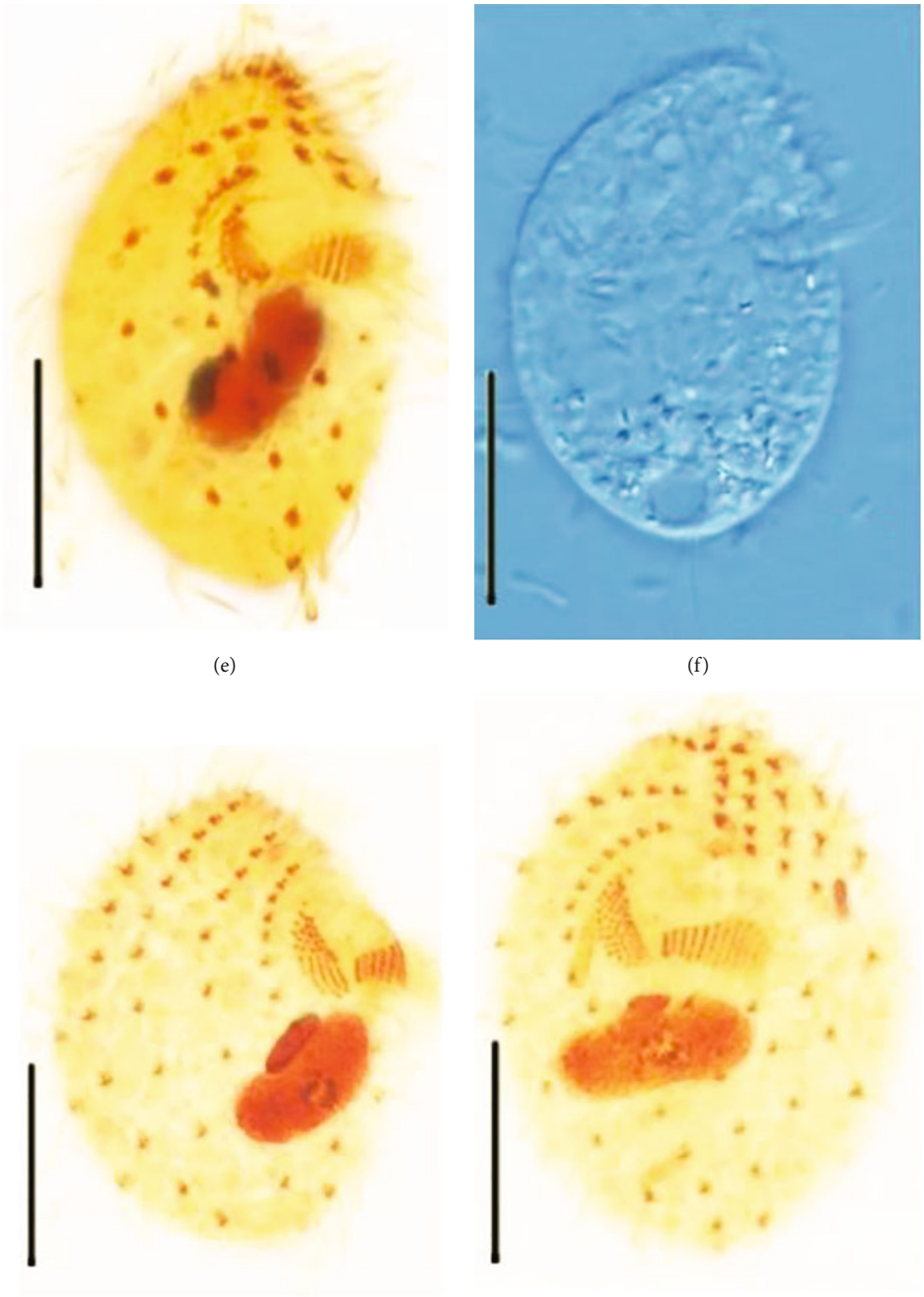

(e) (f)

(g) (h)

Figure 2: Continued.

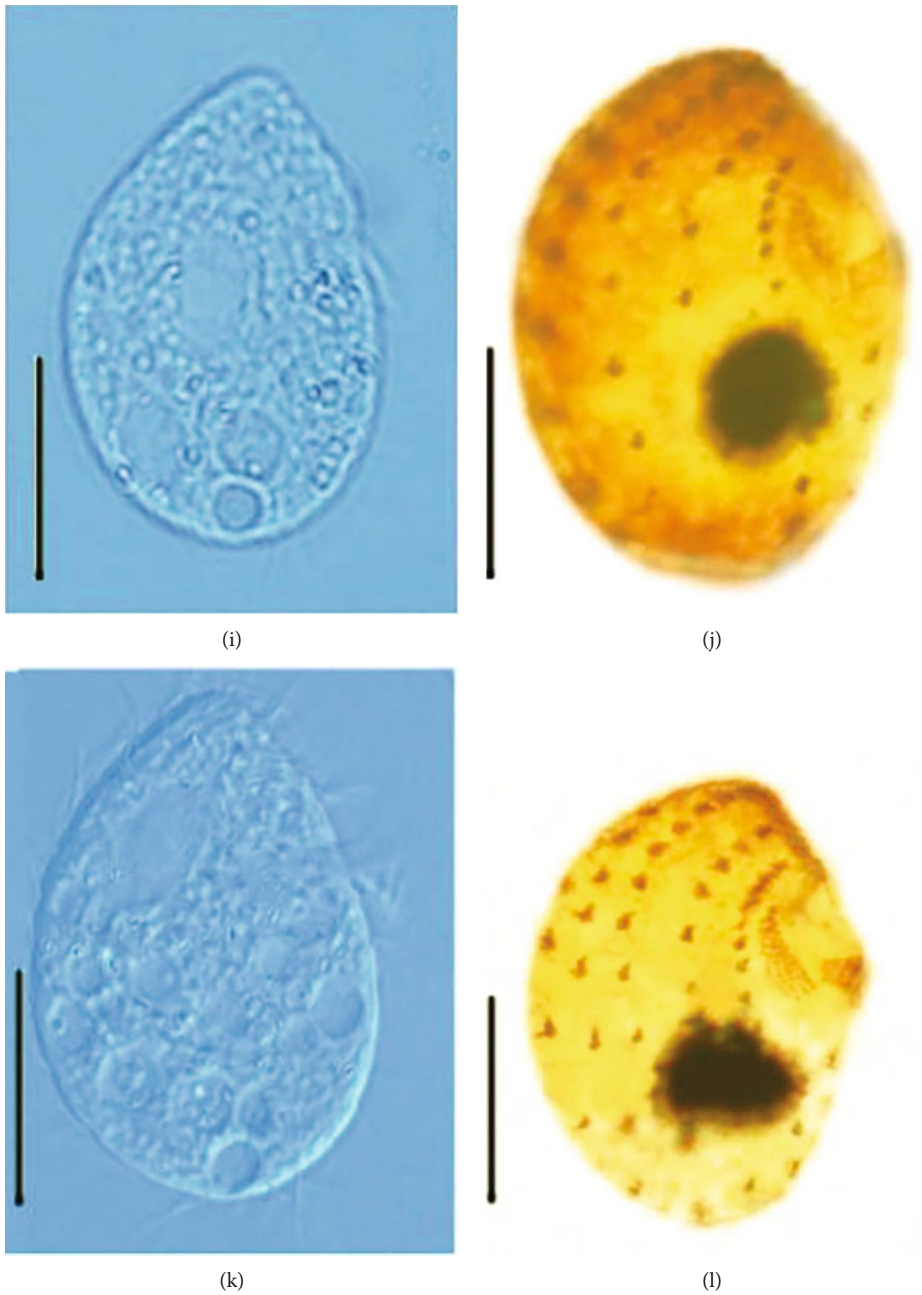

(i) (j)

(k) (l)

Figure 2: Continued.

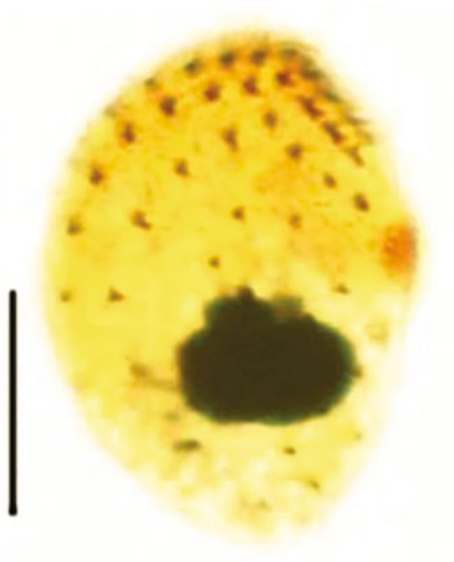

(m)

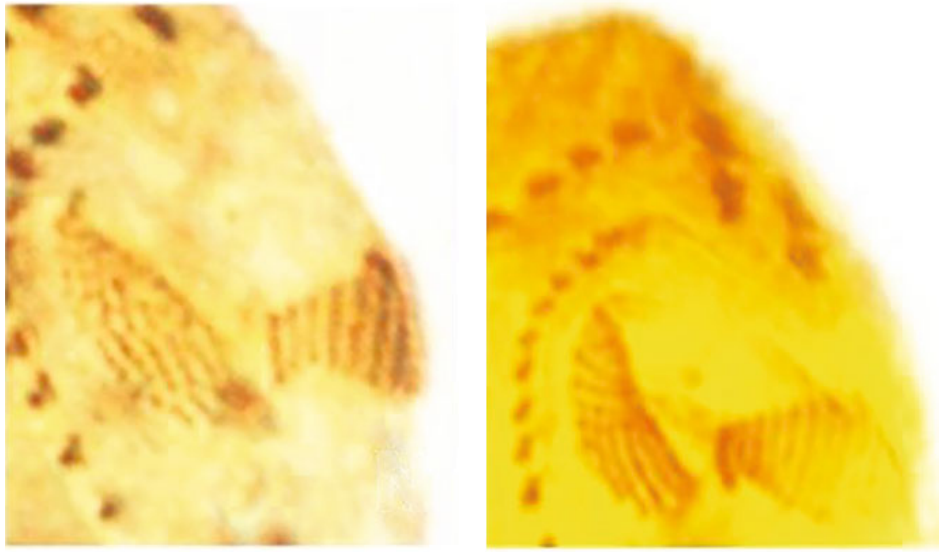

(n) (o)

Figure 2: *Paracolpoda steinii*, photomicrographs from life (a, c, f, i, k) and after silver carbonate staining (b, d, e, g, h, j, l–o). (a, b) Ventral view of a representative individual for population 1. (c)–(e) Ventral view of a representative individual for population 2. (f)–(h) Ventral view of a representative individual for population 3. (i, j) Ventral view of a representative individual for population 4. (k)–(m) Ventral (k, l) and dorsal (m) views to demonstrate the infraciliature for population 5. (n, o) Dorsal views to demonstrate the oral for the population 3. Scale bars = 30 μm (a)–(m).

Bromeliothrix metopoides (100% ML, 0.9 BI). All nine newly sequenced species were clustered within the core of the Colpodea clade. The two newly sequenced species, *Colpoda* compare *grandis* and *C. reniformis*, formed a sister group, which then grouped with *C. henneguyi* and *Bresslauides discoideus*. The newly sequenced *Colpoda harbinensis* n. sp., *C. inflata* pop1, and *C. inflata* pop2 clustered together. The seven *Paracolpoda steinii* sequences, including the five newly sequenced populations, clustered together as a sister group to *Bromeliothrix metopoides* with full support (100% ML, 1.00 BI).

3.3. DNA Barcoding of the Colpoda

3.3.1. The Utility of Cox I Gene Tested for Accurate Identification. The *Cox I* amplification primers MOU08–121 and MOU08–122 (Table 1) yielded a single DNA band of the predicted length (~945 bp) from *Colpoda* compare *grandis*, *C. inflata* pop. 2, *Paracolpoda steinii* pop. 2, and *Paracolpoda steinii* pop. 3 isolates. Therefore, each PCR product was cloned, and the partial *Cox I* sequences were deposited in GenBank under the respective accession numbers OM752200, OM752201, OM752202, and OM752203.

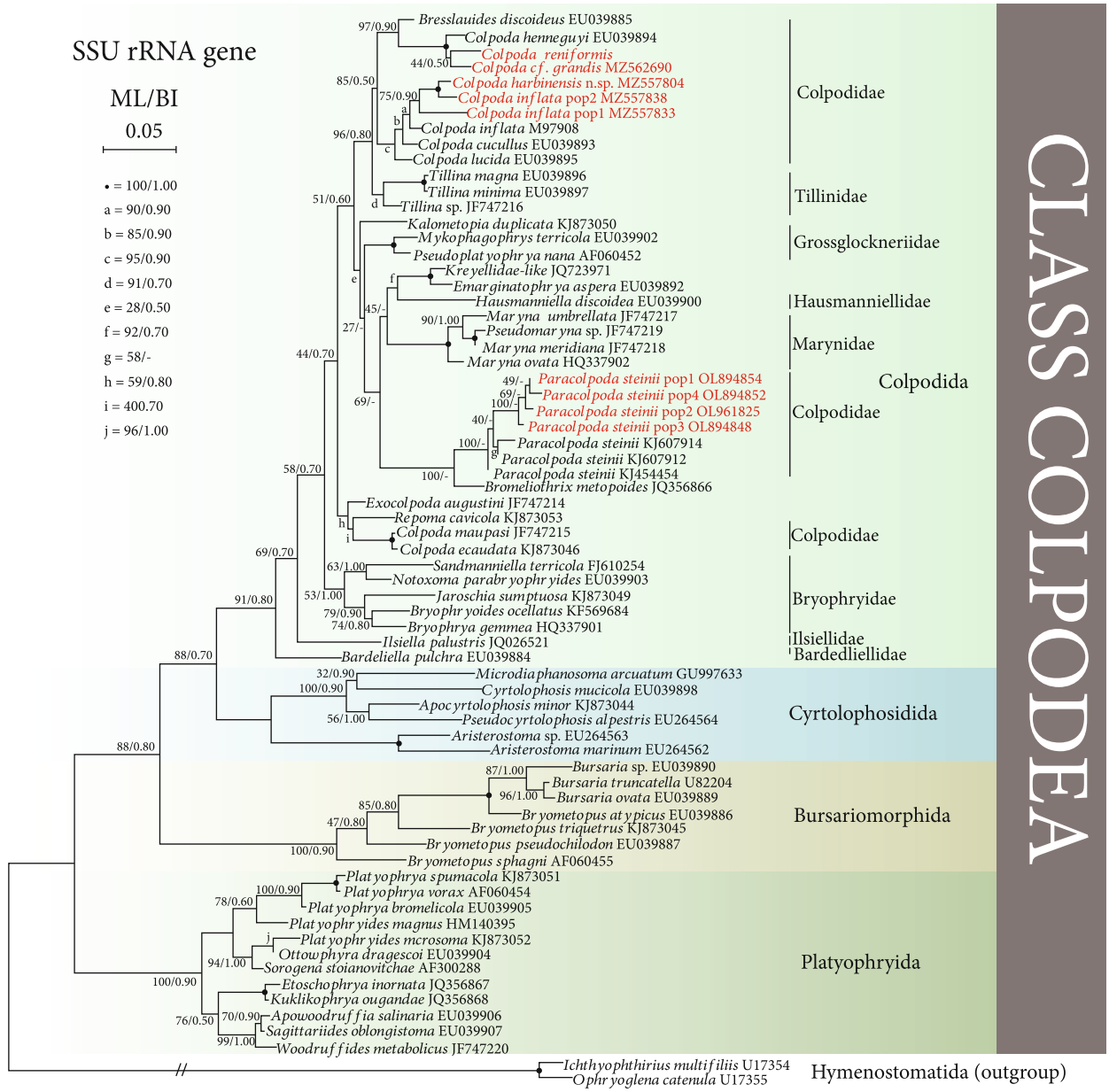

Figure 3: The maximum-likelihood (ML) tree based on the 18S-rRNA gene of major members of the class Colpodea. Newly added sequences in this study are bolded in red type. Node support is shown as ML bootstraps/BI posterior probability. "–" indicates mismatch in topology between Bayesian and ML tree. Fully supported (100%/1.00) branches are marked with solid circles. One long branch has been shortened, as shown by "//", and the other branches are drawn to scale. The scale bar corresponds to 5 substitutions per 100 nucleotide sites.

Their GC contents were 28.56%, 26.42%, 27.87%, and 27.75%, respectively, with sequence differences shown in Figure 4. Base variations between populations of *Colpoda* compare *grandis*, *C. inflata*, and *Paracolpoda steinii* were large, ranging from 12.01% to 14.88%, while the base variation between individuals within the *Paracolpoda steinii* population was small, at 0.35%.

3.3.2. The Utility of β-Tubulin Gene Tested for Accurate Identification. The *β-tubulin* amplification primers 349A and 349B (Table 1) generated a total of 33 DNA sequences of predicted length (~980 bp) from *C. inflata* (populations 1–2), *Paracolpoda steinii* (populations 1–5), and *C. harbinensis* n. sp. isolates. The interspecific genetic distances of *β-tubulin* of *Colpoda* ranged from 0.59% to 8.80%, and intraspecific genetic distances ranged from 0.89% to 5.81%. The TCS network of *β-tubulin* genes revealed the *C. inflata*, the largest difference between pop. 1 and pop. 2 was 60 genetic steps (5a and 2a), while the smallest difference was nine genetic steps (1b and 4). There were large genetic step differences among individuals within the same pop, e.g., 60 genetic step differences between 5a and 4 in pop. 2

Site position / *Cox I*	9	15	18	24	30	45	48	54	66	72	82	84	90	93	96	99	102	126	129	135	150
Colpoda inflata pop2	C	T	C	T	G	T	T	A	T	T	T	A	T	T	A	A	T	T	T	A	T
Colpoda cf. grandis	A	.	T	A	.	A	A	T	A	A	.	.	A	A	T	C	C	A	T	T	G
Paracolpoda steinii pop2	A	.	T	.	A	.	.	T	.	.	A	T	.	.	T	C	.	.	A	T	.
Paracolpoda steinii pop3	A	A	T	.	A	.	.	T	.	.	A	T	.	.	T	C	.	.	A	T	.
Site position / *Cox I*	151	171	174	177	178	186	200	201	204	205	207	219	231	237	240	243	246	247	249	253	255
Colpoda inflata pop2	T	T	T	C	A	A	T	T	T	A	A	A	A	T	T	T	A	T	A	A	T
Colpoda cf. grandis	A	G	.	.	.	T	.	C	G	C	T	.	T	A	C	G	G	.	.	.	.
Paracolpoda steinii pop2	.	A	C	T	G	T	A	.	.	.	.	T	T	.	.	.	.	C	T	G	C
Paracolpoda steinii pop3	.	A	C	T	G	T	A	.	.	.	.	T	T	.	.	.	.	C	T	G	C
Site position / *Cox I*	258	264	285	289	291	297	300	306	309	315	316	317	318	322	324	350	354	359	360	366	376
Colpoda inflata pop2	T	A	T	C	T	C	C	A	T	C	T	C	T	C	T	A	A	T	T	A	T
Colpoda cf. grandis	.	C	C	A	A	T	T	C	A	T	G	.	.	T	A	T	.	.	C	.	.
Paracolpoda steinii pop2	A	.	A	.	.	.	T	T	.	T	.	T	A	T	G	T	G	A	.	T	A
Paracolpoda steinii pop3	A	.	.	.	.	.	T	T	.	T	.	T	A	T	G	T	G	A	.	T	A
Site position / *Cox I*	382	383	387	389	390	393	396	397	398	406	408	411	412	413	414	421	423	433	435	442	447
Colpoda inflata pop2	A	A	A	C	T	A	A	A	A	G	T	T	T	C	T	A	T	C	A	A	A
Colpoda cf. grandis	.	.	.	.	A	.	T	T	C	C	.	C	.	.	.	.	A	G	.	.	T
Paracolpoda steinii pop2	T	C	T	T	.	T	.	.	.	T	A	C	C	A	A	T	.	.	T	C	.
Paracolpoda steinii pop3	T	C	T	T	.	T	.	.	.	T	A	C	C	A	A	T	.	.	T	C	.
Site position / *Cox I*	454	455	456	459	463	464	468	471	474	480	483	485	493	495	507	510	516	519	522	525	528
Colpoda inflata pop2	G	A	A	C	A	G	T	T	T	A	T	A	T	A	T	T	A	C	A	G	A
Colpoda cf. grandis	.	.	.	T	G	A	.	C	A	C	A	.	.	.	A	.	G	T	T	A	T
Paracolpoda steinii pop2	A	C	T	T	G	A	A	.	.	T	.	G	C	T	A	A	.	T	T	A	T
Paracolpoda steinii pop3	A	C	T	T	G	A	A	.	.	T	.	G	C	T	A	A	.	T	T	A	T
Site position / *Cox I*	534	540	543	547	549	561	562	564	573	576	582	585	594	597	598	600	603	609	615	623	624
Colpoda inflata pop2	A	T	A	T	G	A	A	A	A	T	T	T	T	C	A	A	A	A	T	T	T
Colpoda cf. grandis	.	A	.	C	A	T	C	T	G	.	C	A	G	T	.	.	.	T	A	.	A
Paracolpoda steinii pop2	G	A	T	.	A	T	C	T	.	A	.	A	A	T	C	T	T	C	.	C	.
Paracolpoda steinii pop3	G	A	T	.	A	T	C	T	.	A	.	A	A	T	C	T	T	C	.	C	.
Site position / *Cox I*	630	633	636	639	640	641	642	645	654	660	687	688	690	691	692	703	705	709	711	717	720
Colpoda inflata pop2	C	C	T	T	T	C	A	T	A	A	A	T	A	T	C	G	A	G	A	A	A
Colpoda cf. grandis	T	A	C	C	A	G	T	C	G	T	T	.	G	.	.	.	.	.	.	C	T
Paracolpoda steinii pop2	T	T	.	.	.	.	T	.	.	T	.	G	T	G	G	A	T	A	G	T	.
Paracolpoda steinii pop3	T	T	.	.	.	.	T	.	.	T	.	G	T	G	G	A	T	A	G	T	.
Site position / *Cox I*	723	732	747	751	753	756	762	772	775	777	784	786	793	795	798	804	807	810	813	814	816
Colpoda inflata pop2	A	A	T	A	A	T	C	C	A	A	C	T	T	A	A	T	T	T	A	T	A
Colpoda cf. grandis	T	.	.	.	.	.	T	T	C	T	.	.	C	C	T	A	.	A	T	C	T
Paracolpoda steinii pop2	T	T	A	C	T	A	T	T	.	.	A	A	C	T	T	.	A	.	T	.	.
Paracolpoda steinii pop3	T	T	A	C	T	A	T	T	.	.	A	A	C	T	T	.	A	.	T	.	.
Site position / *Cox I*	825	829	831	852	860	867	873	883	885	903	906	915	927	930							
Colpoda inflata pop2	T	C	T	A	G	T	T	C	T	T	T	A	A	A							
Colpoda cf. grandis	.	.	.	.	C	C	A	T	A	A	.	.	T	T							
Paracolpoda steinii pop2	A	A	A	A	.	A	A	T	A	A	A	G	.	G							
Paracolpoda steinii pop3	A	A	A	A	.	A	A	T	A	A	A	G	.	T							

FIGURE 4: *Cox I* sequence comparisons showing the unmatched nucleotides between *Colpoda inflata*, *Colpoda compare grandis*, and *Paracolpoda steinii*. Nucleotide positions are given at the top of each column. Matched sites are represented by dots (.).

(Figure 5(a)). Within *Paracolpoda steinii*, pop. 3 (7) and pop. 5 (11b) differed by 69 genetic steps, while pop. 4 (8a) differed from pop. 2 (3a) and pop. 3 (6a) by only one genetic step. In addition, there were large genetic step differences among the offspring individuals produced from the same individual by monoclonal cultures, such as 10 and 9 genetic step differences between 3a and 3b and 4a and 4b in pop. 2, respectively (Figure 5(b)).

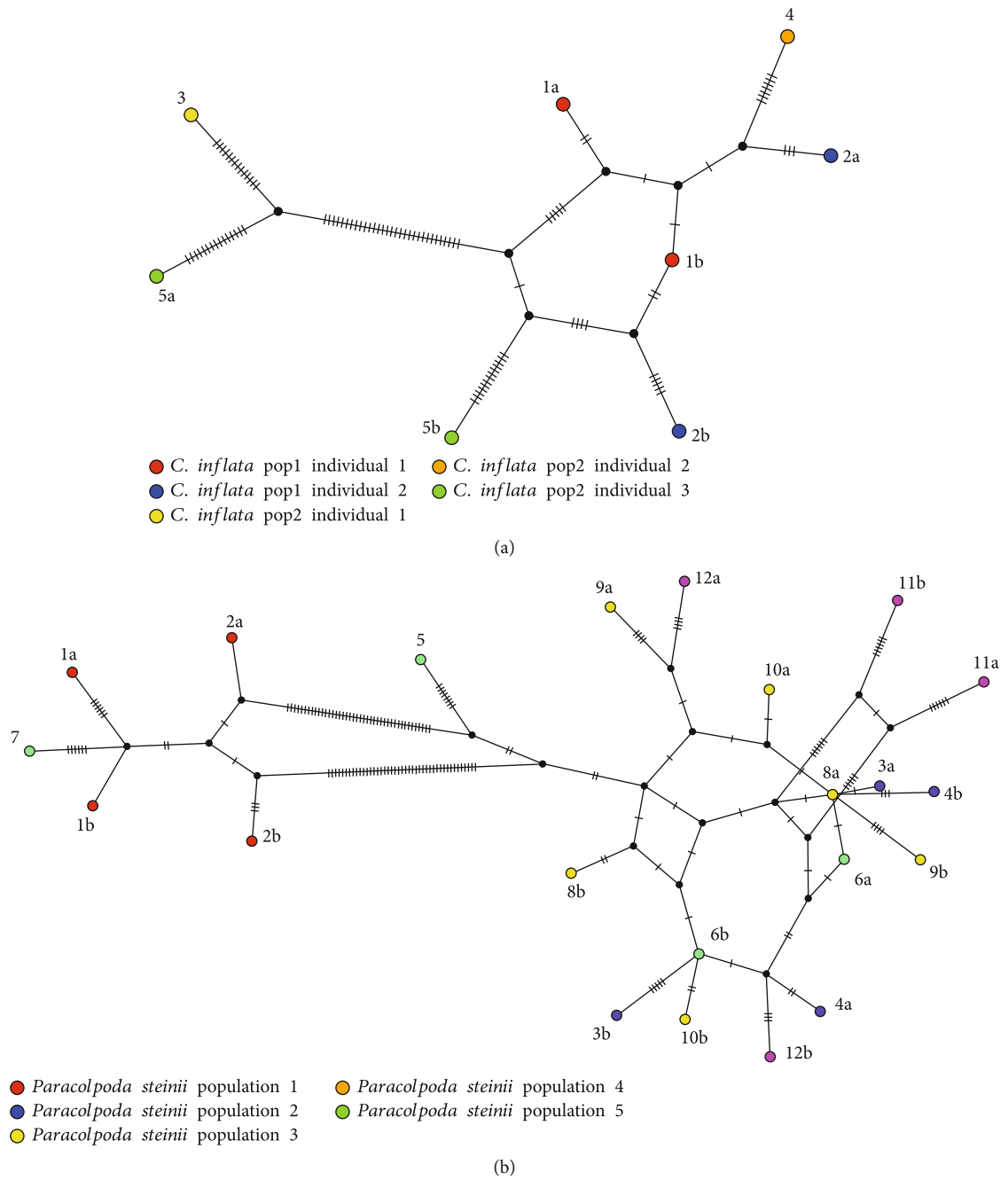

Figure 5: TCS network of the *β-tubulin* gene of *Colpoda inflata* (a) and *Paracolpoda steinii* (b). Black orbs represent intermediate haplotypes that were not sampled, and the lines between individual haplotypes represent the number of nucleotide substitutions. Numbers represent different individuals, and the letter after the number represents the clone of that individual.

3.4. Detection and Identification Using FISH. Our five probes were evaluated with the probe match tool in the ARB software package, revealing that they were specific to *Colpoda* (Table 3). There are one to six mismatches between the probes of different *Colpoda* species. After conducting fluorescence in situ hybridization with each of the five probes, *Colpoda* compare *grandis*, *C. harbinensis* n. sp., *Paracolpoda steinii* pop. 4, *P. steinii* pop. 5, *C. inflata* pop. 1, and *C. inflata* pop. 2 all exhibited red fluorescent signals (Figures 6(a)–6(h) and 6(m)–6(p)), clearly distinguishable from the faint autofluorescence signals achieved with negative-control hybridizations using the TSBs probe to hybridize the untargeted ciliates *C. reniformis* (Figures 6(i) and 6(j)) and *Coleps hirtus* (Figures 6(k) and 6(l)). FISH also provided some morphological information such as body shape, macronucleus shape, and macronucleus number (Figures 6(b), 6(d), 6(f), 6(h), 6(n), and 6(p)). The signal intensity became weaker when the formamide (FA) concentration increased in the hybridization buffers, and the fluorescence signals with more than 10% FA were weaker than

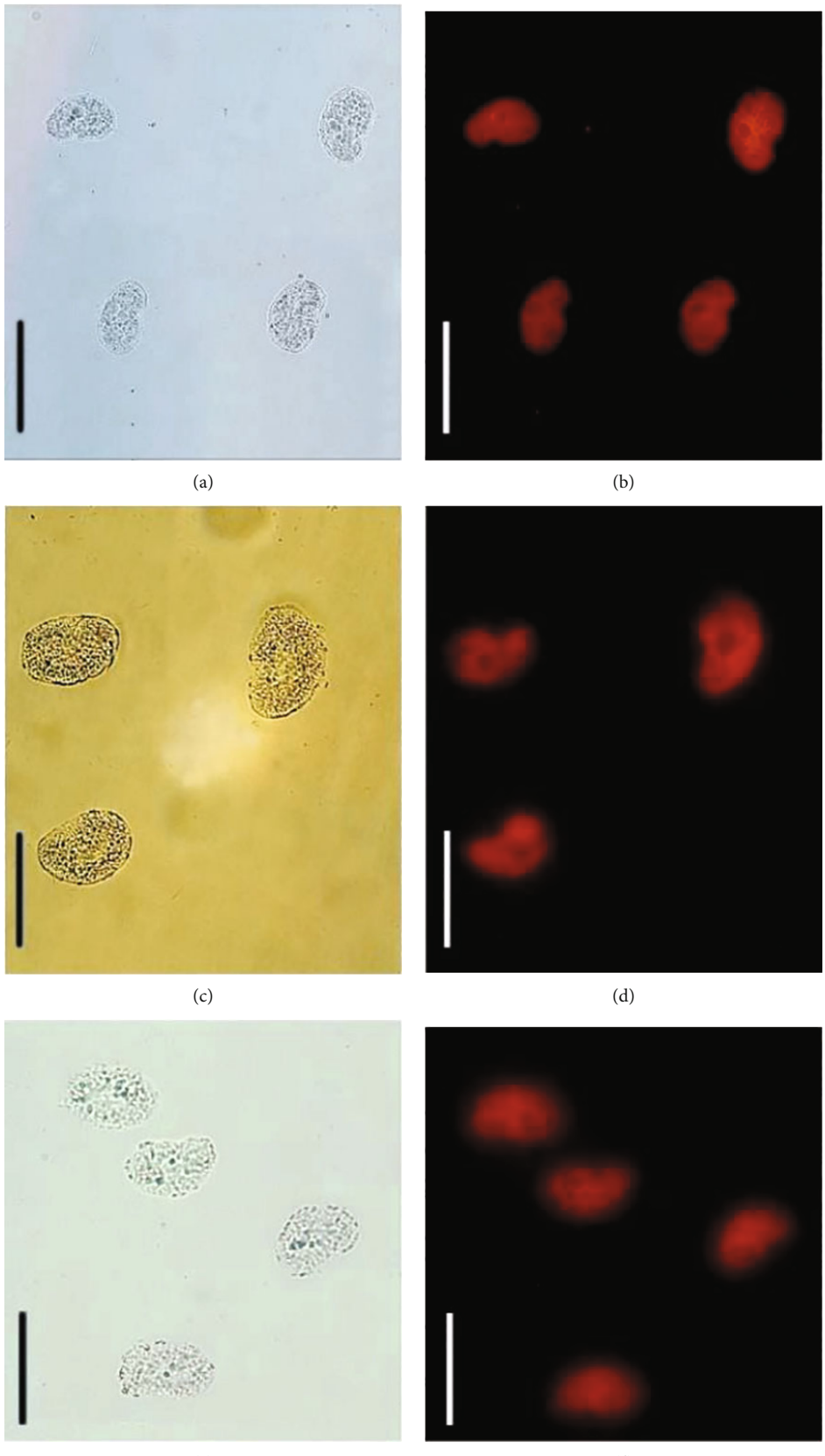

(a) (b) (c) (d) (e) (f)

Figure 6: Continued.

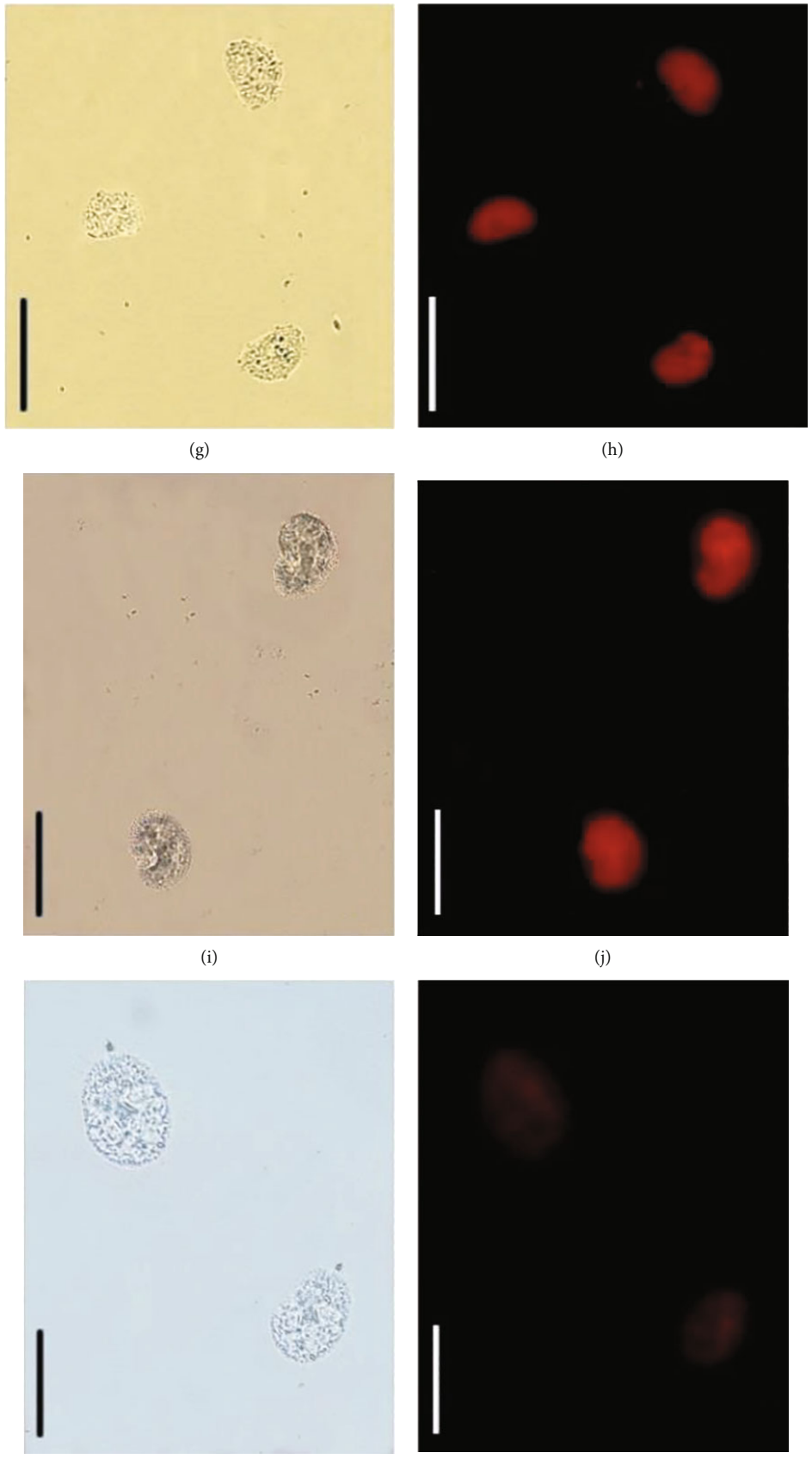

(g) (h) (i) (j) (k) (l)

Figure 6: Continued.

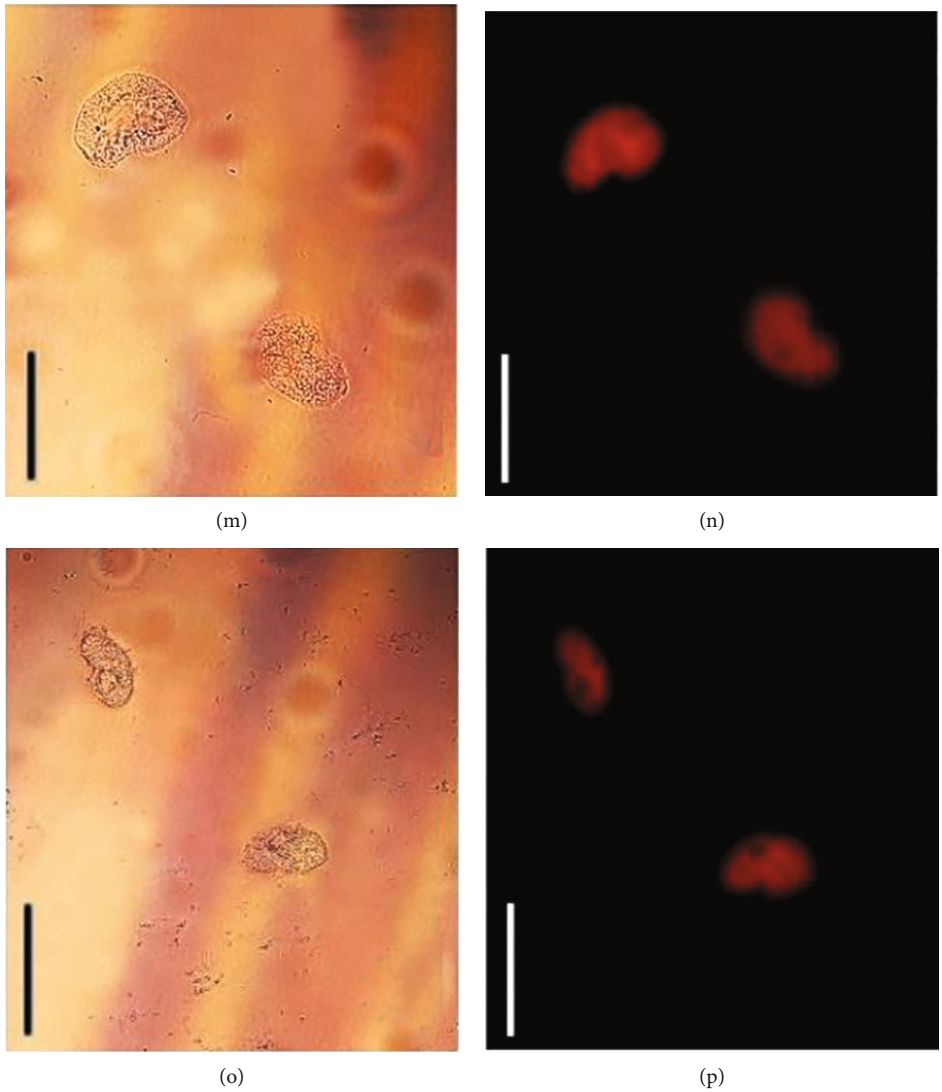

Figure 6: Fluorescence in situ hybridization staining of *Colpoda* species (a–j, m–p) and other test ciliates (k, l). (a, b) *Colpoda* compare *grandis* in vivo (a) and stained with the probe YdaA (b). (c, d) *Colpoda harbinensis* n. sp. in vivo (c) and stained with the probe BBxA (d). (e)–(h) *Paracolpoda steinii* populations 4 and 5 in vivo (e, f) and stained with the probe TSBS (g, h). (i, j) *Colpoda reniformis* in vivo (i) and stained with the probe TSBS (j). (k, l) *Coleps hirtus* in vivo (k) and stained with the probe TSBS (l). (m, n) *C. inflata* population 1 in vivo (m) and stained with the probe GRA (N). (o, p) *C. inflata* population 2 in vivo (o) and stained with the probe ZL (p). Scale bars = 400 μm (a, b); 90 μm (c, d); 90 μm (m–p, k, l); 70 μm (i–l); 20 μm (i, j).

those of the positive control. Therefore, 10% of formamide in the hybridization was the optimal concentration for the stringency of our probes.

3.5. Establish of New Species. Here are the following classifications of new species:

Class: Colpodea Small and Lynn, 1981
Order: Colpodida Puytorac et al., 1974
Family: Colpodidae Bory De St. Vincent, 1826
Genus: *Colpoda* Müller, 1773
Species: *Colpoda harbinensis* sp. nov

Diagnosis is as follows: size in vivo approximately 75 – 90 × 50 – 66 μm, reniform in outline; narrower toward anterior and wider towards posterior; one spherical macronucleus, micronucleus sometimes nonexistent; 11–15 somatic kineties; five or six postoral kineties; left oral polykinetid elongate elliptic, composed of an average of 13 kineties; a few pronounced diagonal grooves present; and soil habitat. Type locality is as follows: soil from Hulan Beet Research Institute of Heilongjiang University (45°59′47″N, 126°38′18″E), Harbin, Heilongjiang province, northeastern China. Type specimens were as follows: the slide containing the holotype specimen (Figures 7(d) and 7(e)) and a paratype slide (registration number SYM–2020301011–02) are deposited in the Laboratory of Protozoology, Harbin Normal University. ZooBank registration was as follows: present work: urn:lsid:http://zoobank.org/:pub:2E33F1C0–CF47–4126–B317–C3505BC41C46. New species: urn:lsid:zoobank. Org:act:485F1 A9C–4078–4F62–8C9C–06A6527EE730. Etymology was as follows: the species group name "harbinensis" indicates

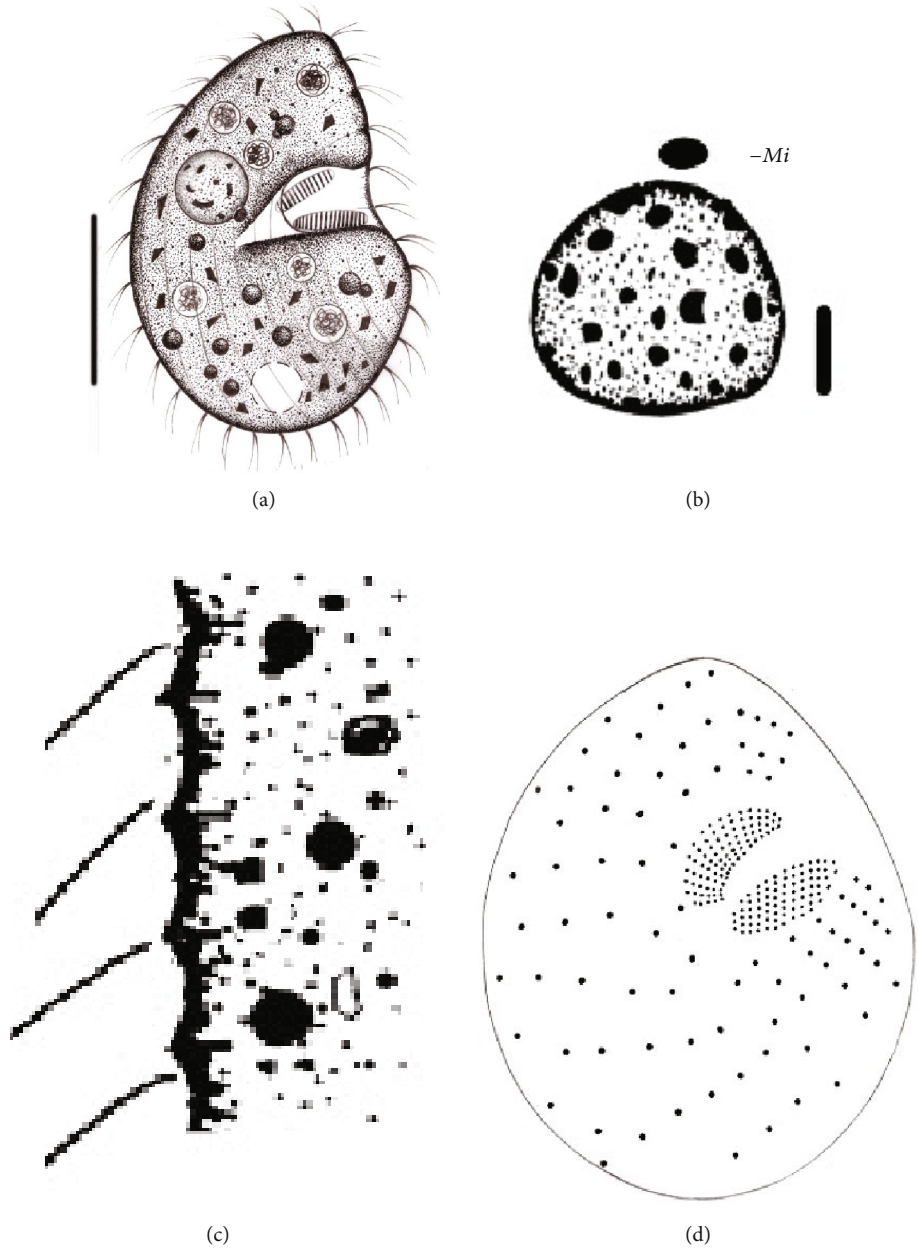

(a) (b)

(c) (d)

Figure 7: Continued.

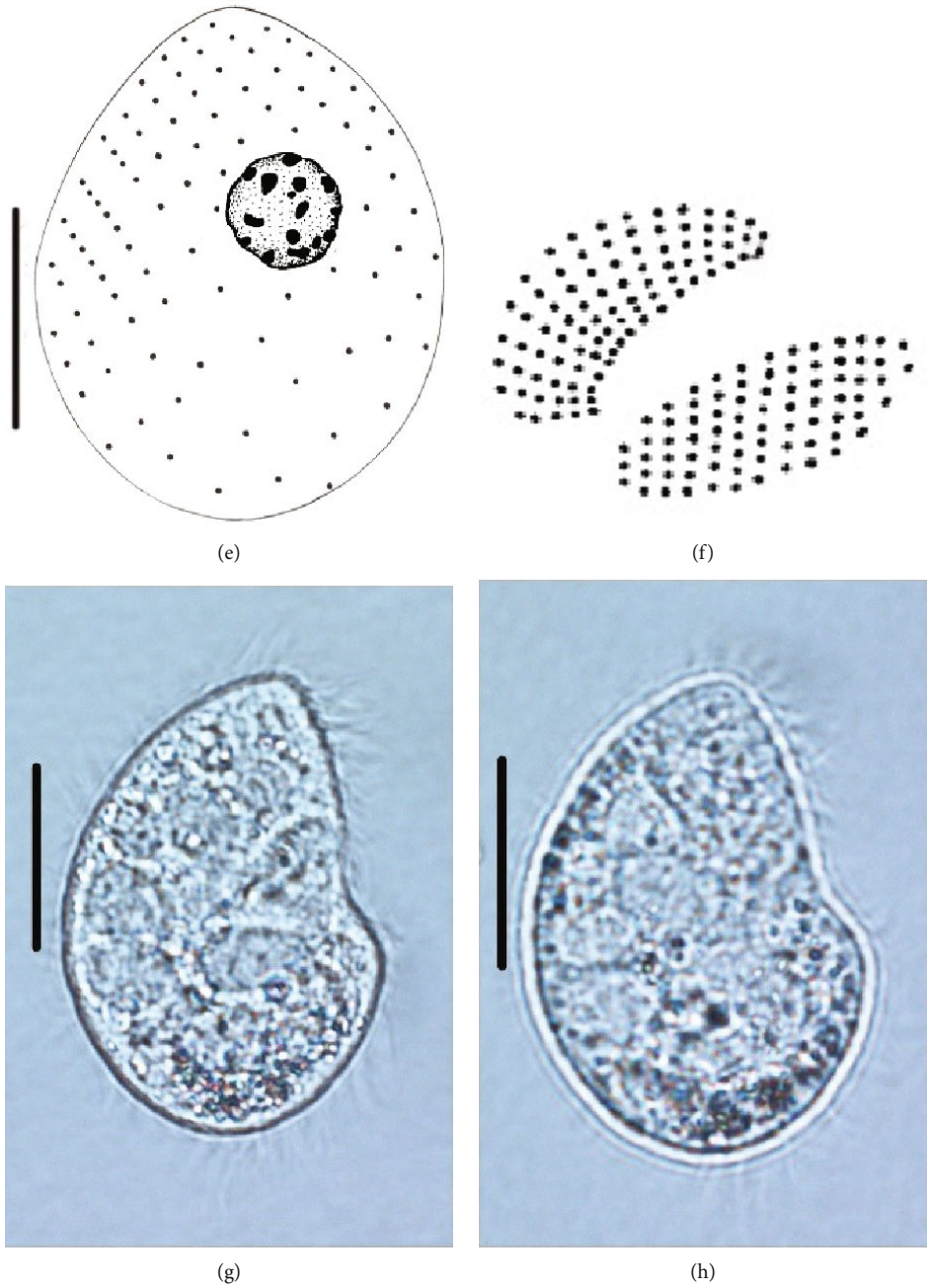

(e) (f)

(g) (h)

Figure 7: Continued.

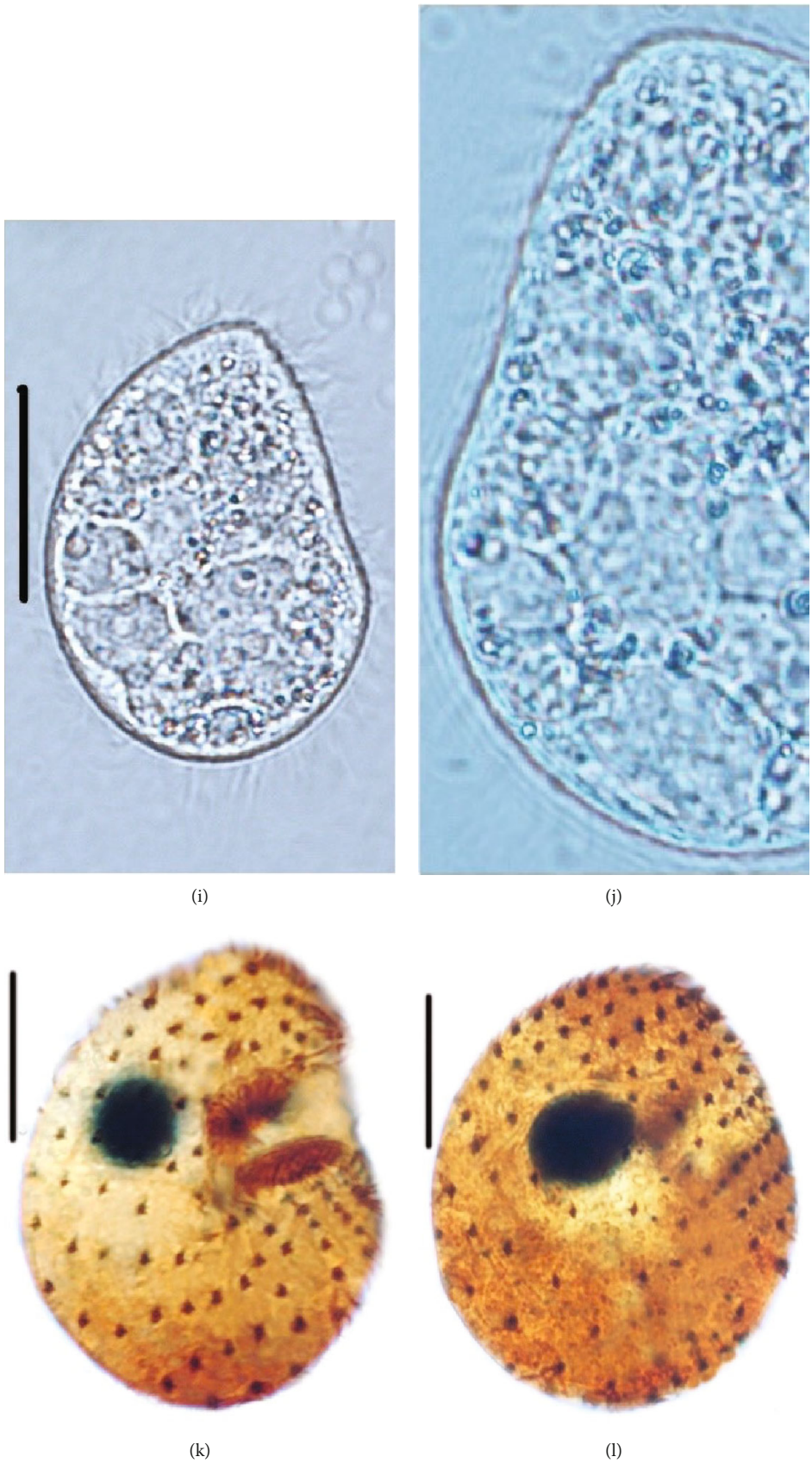

(i) (j)

(k) (l)

Figure 7: Continued.

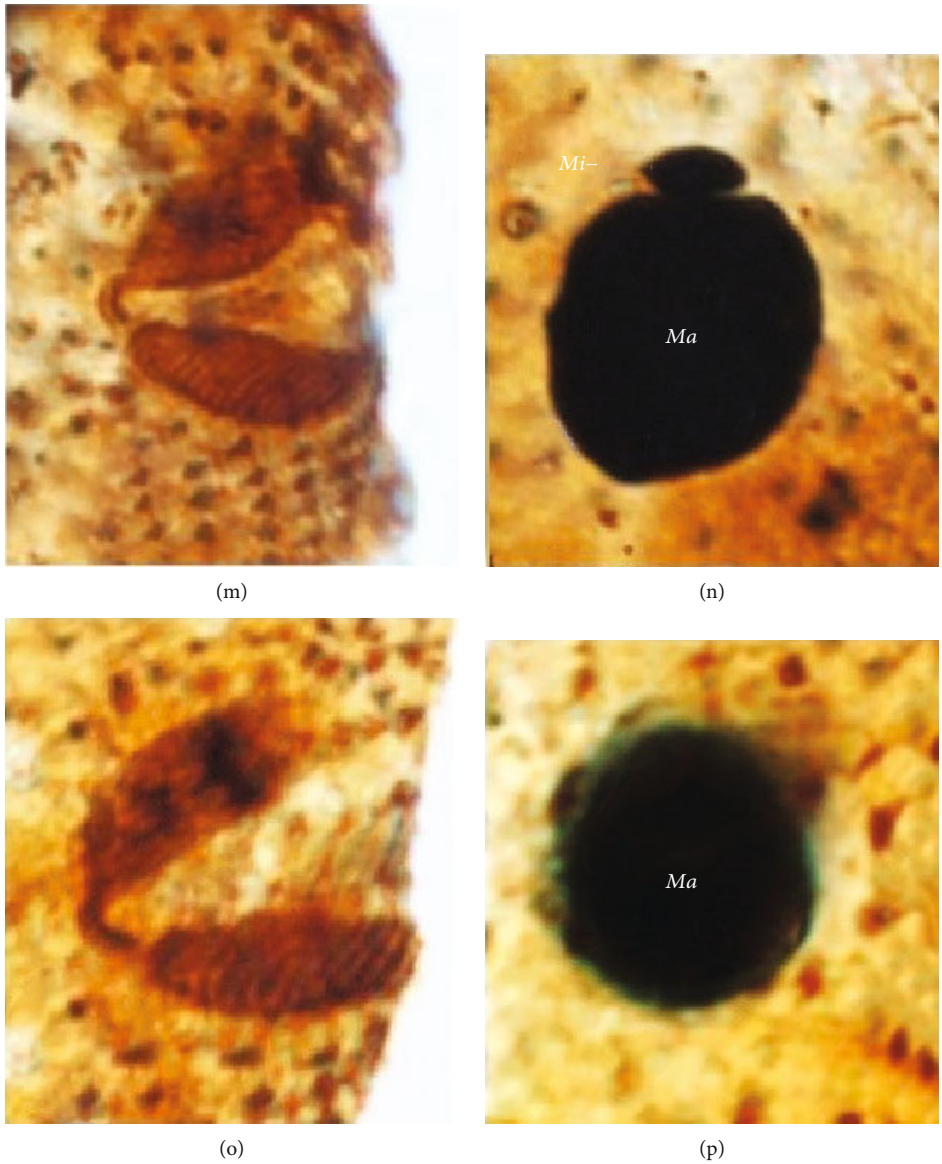

Figure 7: *Colpoda harbinensis* n. sp., morphology from life (a) and after silver carbonate staining (d, e) and photomicrographs from life (g–j) and after silver carbonate staining (k)–(p). (a) Ventral view of a representative individual. (b) Part of pellicle, to show extrusomes. (c) Macronucleus and micronucleus. (d, e) Ventral (d) and dorsal (e) views of the holotype specimen, to show the whole infraciliature. (f) Details of the oral apparatus. (g)–(i) Ventral views of representative individuals, to show different body shapes. (j) Dorsal views, to mark the diagonal grooves. (k, l) Ventral (k) and dorsal (l) view to demonstrate the infraciliature. (m)–(p) Dorsal views, to demonstrate the oral (m, o) and nuclear apparatus (n, p). Ma: macronuclear nodules; Mi: micronuclei. Scale bars = 30 μm (a, d, e, g–i, k, l); 5 μm (b).

that this species was isolated from a sampling site in Harbin, Heilongjiang province, northeastern China.

3.5.1. Morphological Description (Figure 7 and Table 4). Cell has a size approximately 75 – 90 × 50 – 66 μm in vivo, usually about 80 × 60 μm, length to width ratio close to 1.5 : 1 in life (Table 4): reniform in outline (Figures 7(a), 7(d)–7(i), 7(k), and 7(l)) and straight keel and distinctly projecting ventrally, with four or five notches (Figures 7(a) and 7(g)–7(j)). Buccal field occupies approximately one fifth of body length, funnel opening about 7 μm wide in vivo. Cytoplasm colorless contains several minute (<0.5 μm) crystals, mainly concentrated in the lower right corners, glistening under interference contrast illumination; only a few pronounced diagonal grooves were observed (Figures 7(g)–7(i)). Macronucleus globular to slightly ellipsoid, 18.7 × 15.6 μm on average, was generally above mid-body right of median (Figures 7(a), 7(b), 7(e), 7(n), and 7(p); Table 4). Micronucleus ellipsoid-shaped was attached to macronucleus, about 2 × 1 μm in vivo (Figures 7(b) and 7(n); Table 4), sometimes nonexistent. Contractile vacuole was slightly ahead of posterior end, approximately 4 μm in diameter during diastole (Figures 7(a) and 7(g)–7(i)), without tubular drainage pore. Cortex inconspicuous, flexible, extrusomes was recognizable

Table 4: Morphometric characterization of *Colpoda harbinensis* n. sp.

Character	Min	Max	Mean	M	SD	CV	*n*
Body length, μm	75.0	91.0	83.4	82.0	29.57	0.35	11
Body width, μm	50.0	66.0	57.5	55.1	20.46	0.36	11
Macronucleus, number	1.0	1.0	1.0	1.0	0.0	0.0	11
Macronucleus length, μm	12.7	24.0	18.7	18.9	6.33	0.34	9
Macronucleus width, μm	10.7	20.2	15.6	15.1	5.34	0.34	9
Micronucleus, number	0.0	1.0	0.27	0	0.16	0.58	11
Micronucleus length, μm	7.5	8.8	2.66	0	1.54	0.58	9
Micronucleus width, μm	2.5	4.4	1.19	0	0.70	0.59	9
Distance from anterior end to distal edge of vestibulum, μm	25.2	34.1	29.1	28.4	9.77	0.34	9
Distance from anterior end to proximal edge of vestibulum, μm	37.8	46.7	41.3	40.4	13.84	0.33	9
Somatic kineties, number	11.0	15.0	12.8	13.0	4.32	0.33	9
Postoral kineties, number	5.0	6.0	5.44	5.0	1.82	0.33	9
Left lateral kineties, number	5.0	7.0	5.78	6.0	1.94	0.34	9
Left polykinetid length, μm	22.7	35.3	29.9	30.3	10.73	0.36	8
Left polykinetid width, μm	5.7	8.8	7.5	7.5	2.68	0.36	8
Left polykinetid, number	12.0	13.0	12.6	13	4.76	0.38	7
Right polykinetid length, μm	18.2	28.3	24.0	24.2	8.58	0.36	8
Right polykinetid width, μm	6.8	10.6	9.0	9.1	3.22	0.36	8

Data from silver carbonate-stained specimens. CV, coefficient of variation (%); M, Median; Max, maximum; Mean, arithmetic mean; Min, minimum; n, number of specimens; SD, standard deviation.

in vivo (Figures 7(c) and 7(i)). Cytoplasm contains numerous granules, variably sized bacteria-filled food vacuoles, and crystals (Figures 7(a) and 7(g)–7(j)) and moderately fast spiral movement on a substrate and rapid spiral swimming in water.

Typical *Colpoda* ciliature pattern was as follows: somatic cilia (approximately 8 μm long) was closely arranged (Figures 7(a) and 7(g)–7(i); Table 4) and was densely arranged in the anterior part of the oral cavity, distinctly spiral, and roughly "S"-shaped, ranging in number from 11 to 15, each composed of monokinetids (Figures 7(a), 7(d), 7(e), 7(k), and 7(l); Table 4). Left oral polykinetid situated on elongate elliptic and consisting of an average of 13 minute kineties: five postoral kineties (Table 4; Figures 7(a), 7(d), and 7(k)).

3.5.2. Gene Sequence Data. The SSU rDNA sequence of *Colpoda harbinensis* sp. nov. has been deposited in the GenBank database with the accession number, length, and G + C content as follows: MZ557804, 1716 bp, and 44.23%.

4. Discussion

4.1. Comparison of Known Species with Original Descriptions

4.1.1. Colpoda reniformis Kahl, 1931. Our population of *C. reniformis* is similar to previous populations, as they share a distinctly nephrogenic body shape in vivo and an ellipsoid macronucleus between their vestibulum and dorsal side but is distinct in their large body size (123 – 130 × 85 – 95 μm in the present study vs. 90–100 μm) and absence of micronucleus (vs. presence in the previous populations [30, 55].

4.1.2. Colpoda Compare grandis Smith, 1899. Colpoda compare *grandis* has many features that are similar to those of *C. grandis*: body reniform in vivo (about 2 : 1) with a distinct indentation at its vestibular entrance sometimes absent, laterally flattened, no postoral sack, contractile vacuole, cytopyge near its posterior end, extrusomes conspicuous and numerous, left oral polykinetid on the vestibular bottom, and elongate square [30, 56]. However, *Colpoda* compare *grandis* differs from *C. grandis* by the shape of the macronuclei (round vs. distinctly oval in *C. grandis*; Smith [56]). However, the morphology of macronucleus alone is not sufficient to distinguish *Colpoda* species. Considering the slightly variable shape of the macronucleus in *Colpoda*, the insufficient number of specimens investigated in this study, and the close phylogenic relationship with *C. grandis* based on the SSU-rRNA gene sequences, we temporarily identify our isolate as *Colpoda* compare *grandis*.

4.1.3. Colpoda inflata Stokes, 1884. Both the two Chinese populations of *C. inflata* have typical "L"-shaped body with a marked preoral narrowing and a hemispherical postoral portion, similar numbers of somatic kineties, and postoral kineties with those of previous studies [57–59]. The body size of pop. 1 did not differ much from previous studies; although, the body size of pop. 2 was much larger (40 – 60 μm × 30 – 50 μm in the previous populations compared to 85 – 88 μm × 65 μm in the present study) [59].

4.1.4. Paracolpoda steinii Maupas, 1883. Compared with the previous studies, the four Chinese populations of *P. steinii* are similar in the following characteristics: dikinetid, two longer caudal cilia, a distinctly ellipsoidal macronucleus

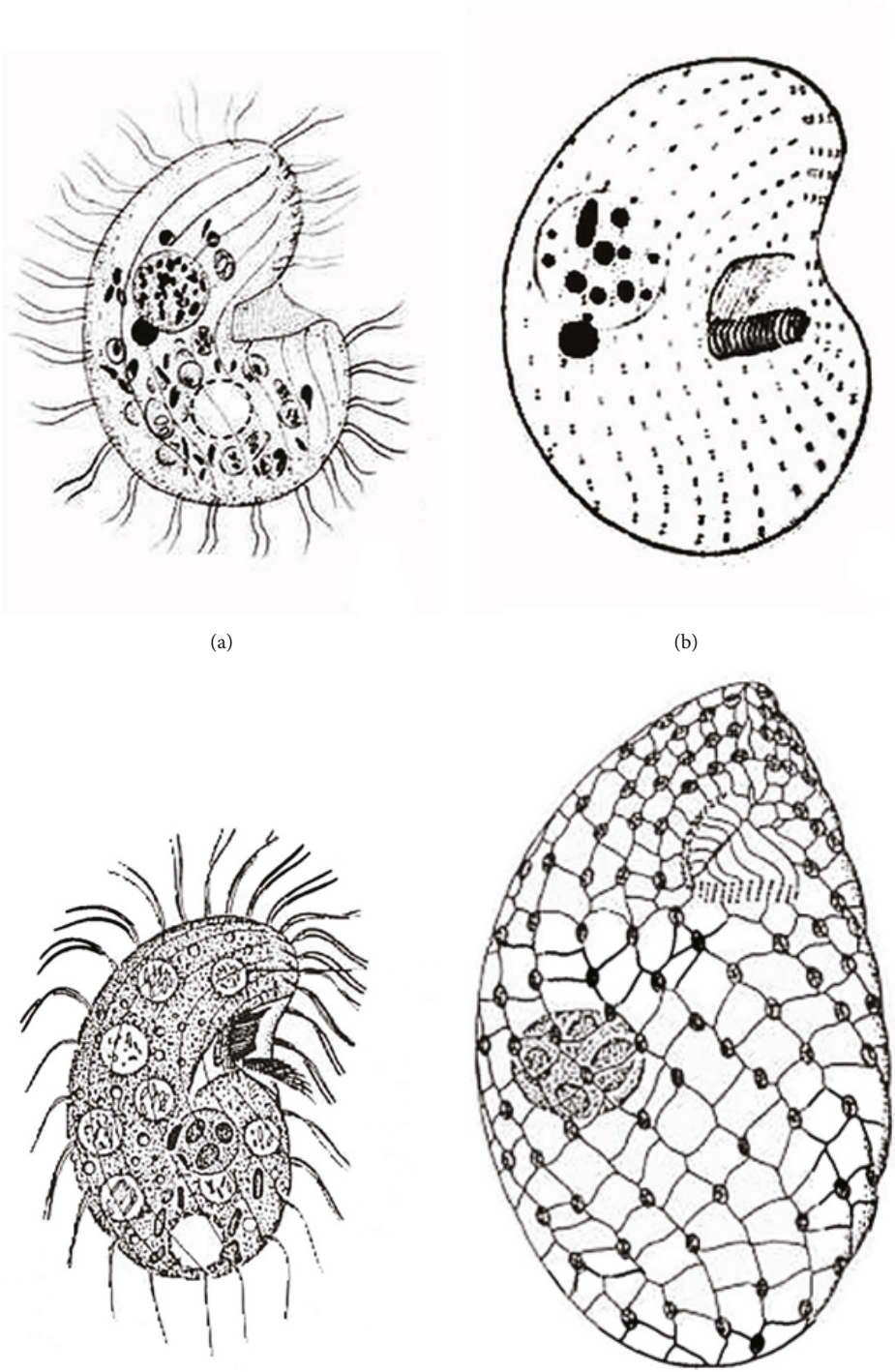

(a) (b)

(c) (d)

Figure 8: Continued.

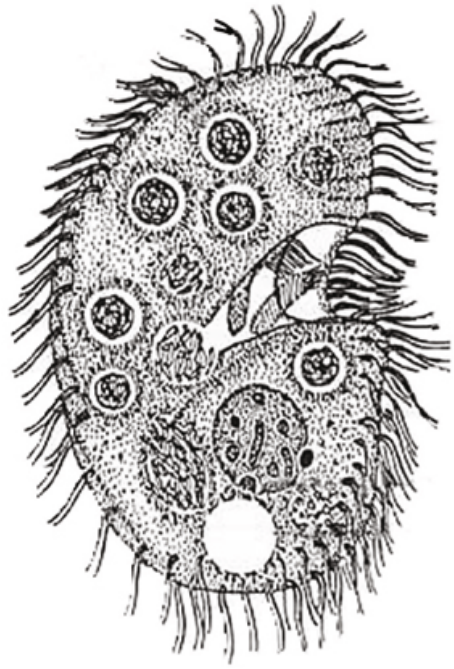

(e)

(f)

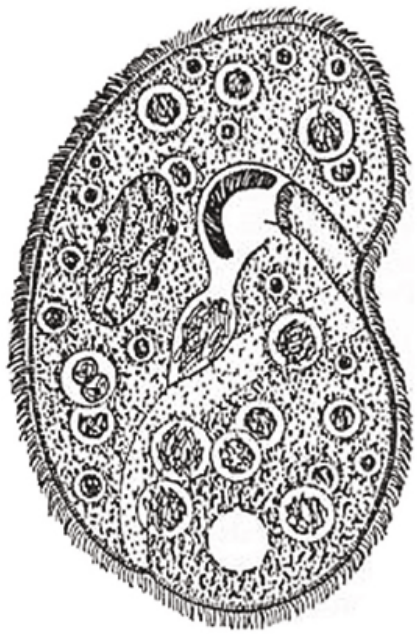

(g)

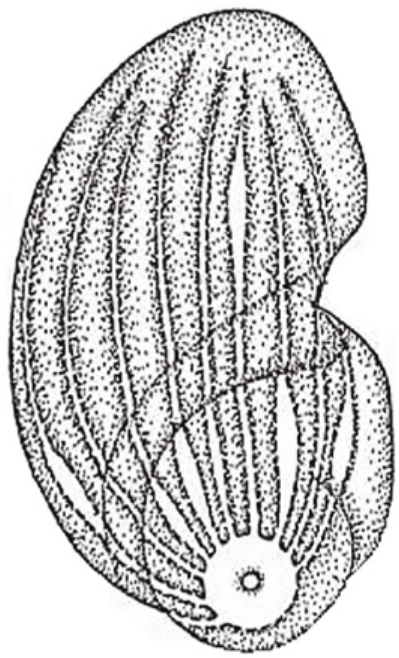

(h)

Figure 8: Continued.

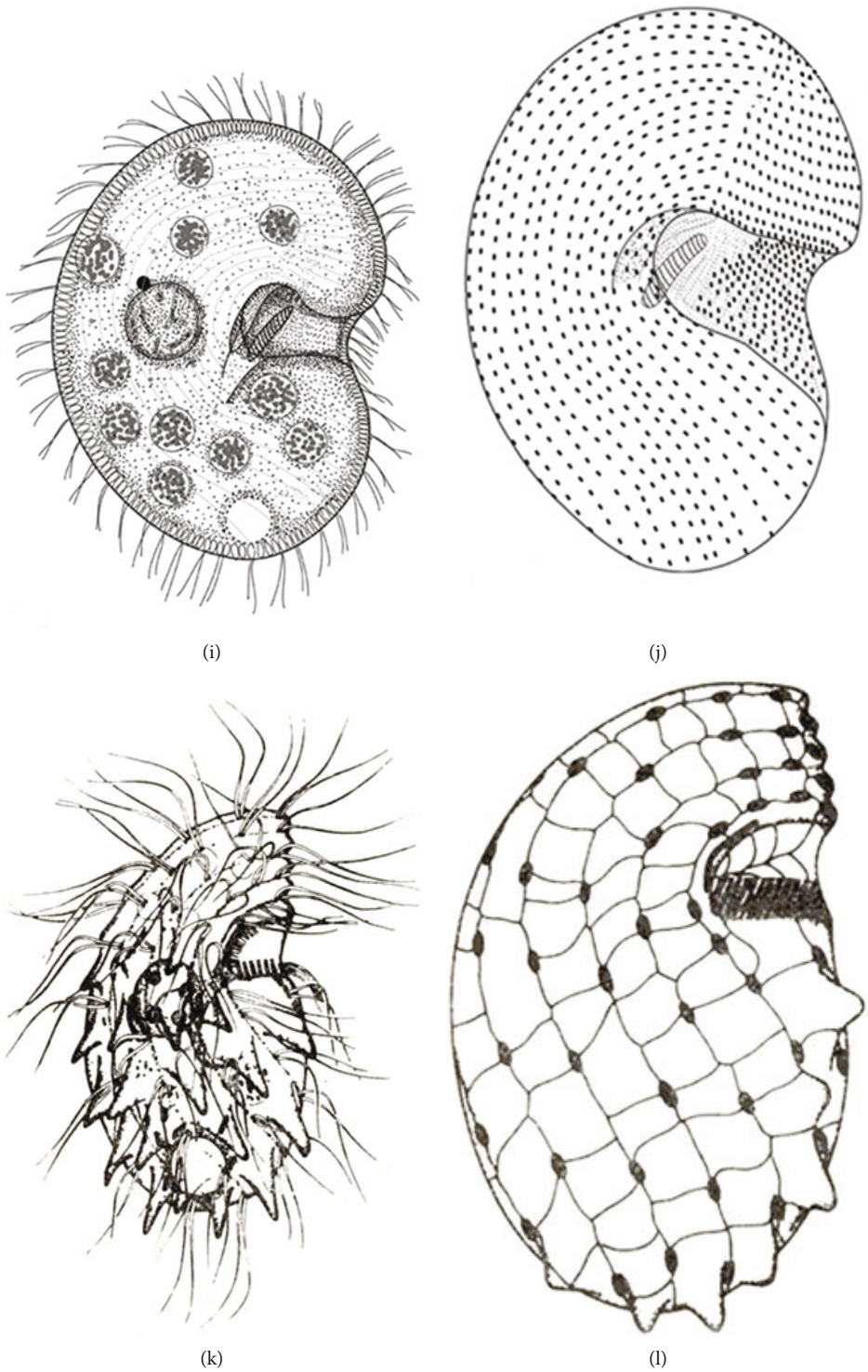

(i) (j)

(k) (l)

Figure 8: Continued.

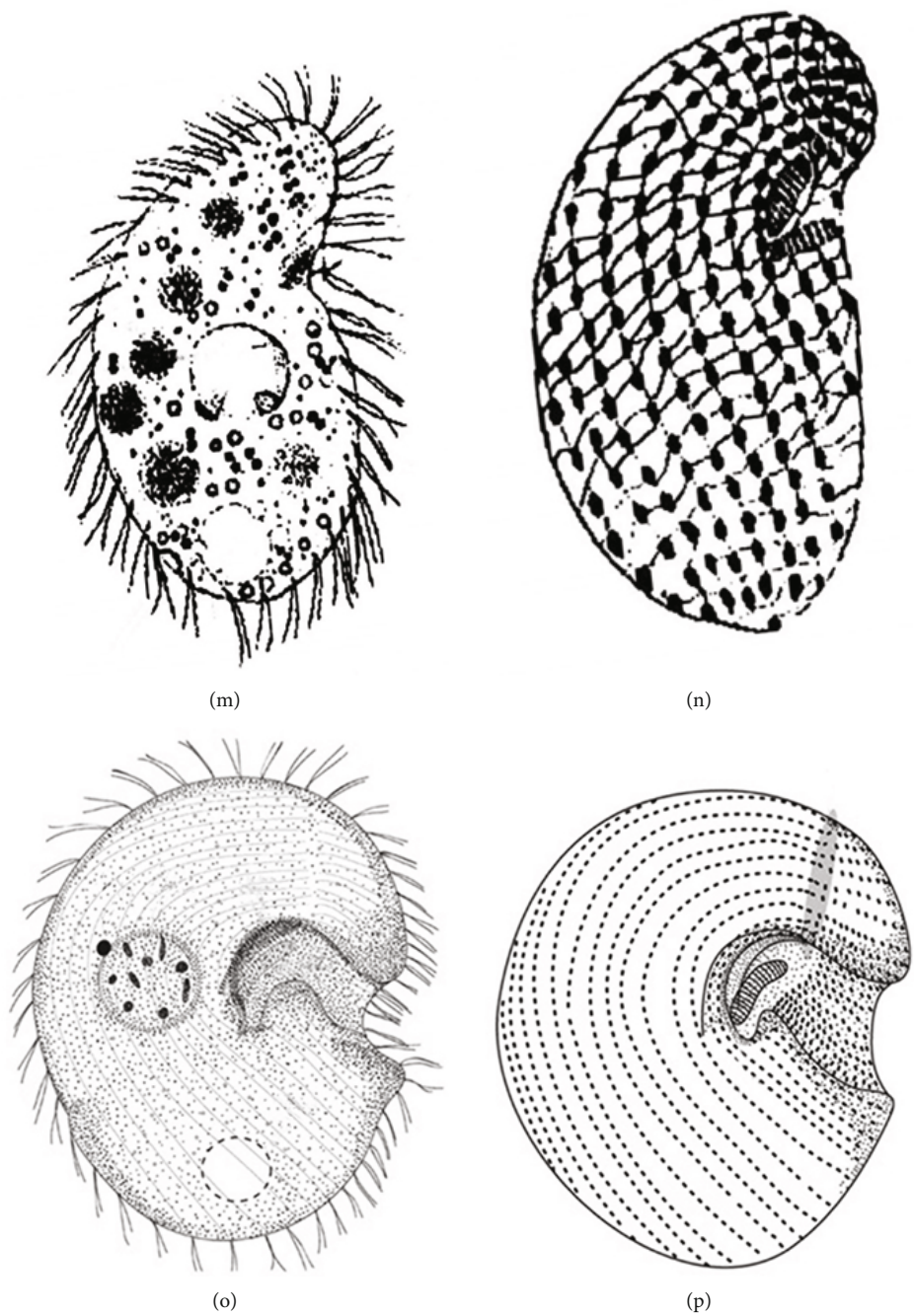

(m) (n)

(o) (p)

Figure 8: Continued.

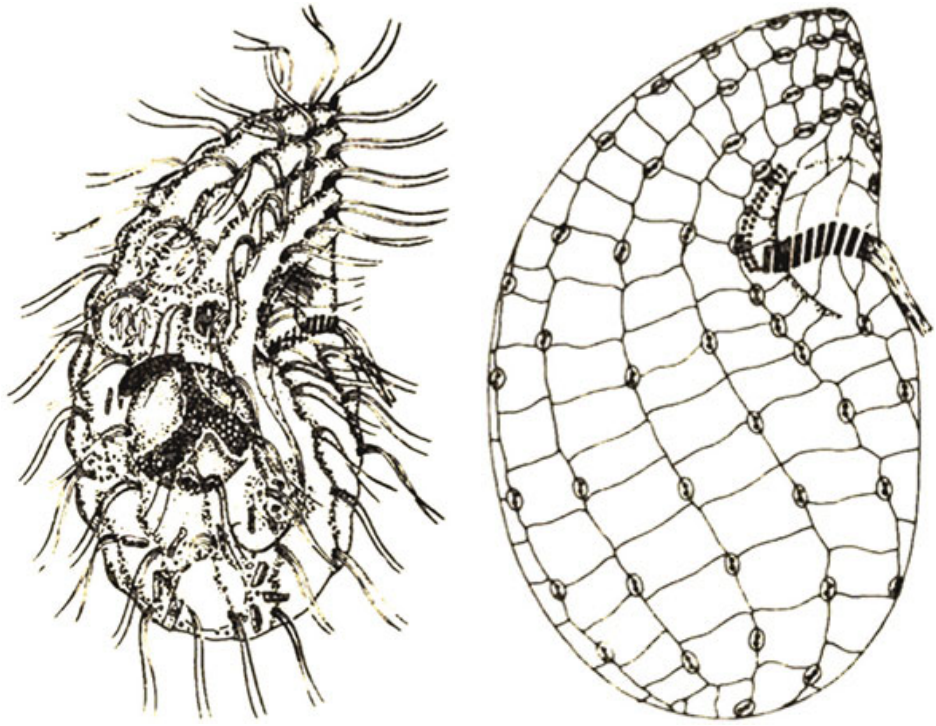

(q) (r)

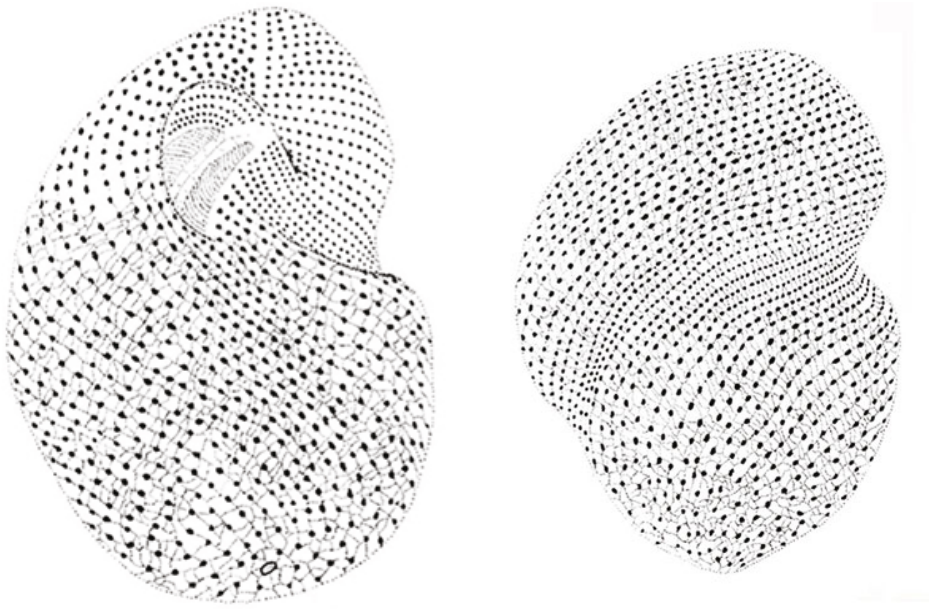

(s) (t)

Figure 8: Continued.

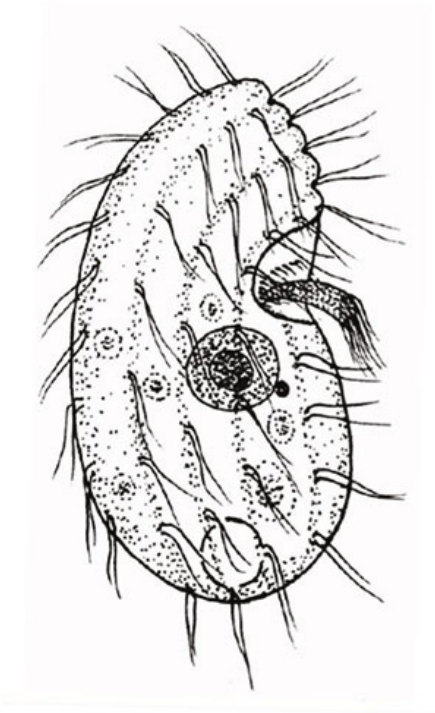

(u)

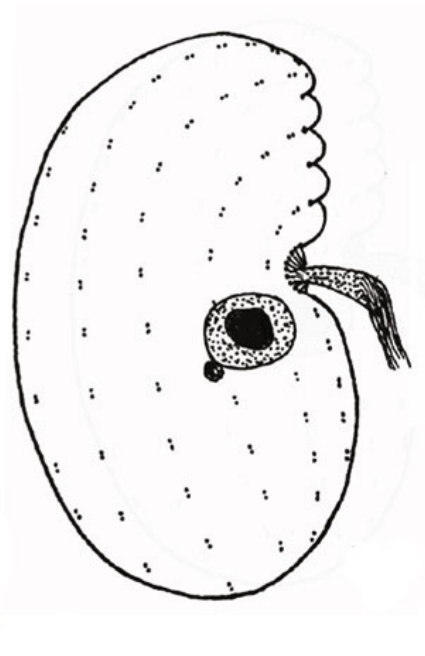

(v)

(w)

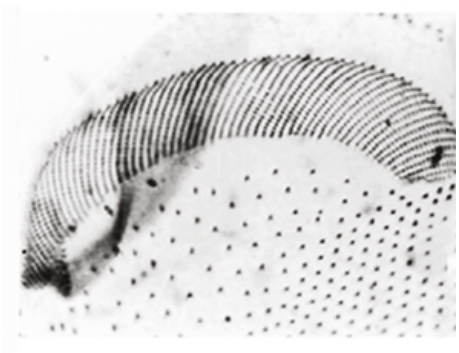

(x)

Figure 8: Continued.

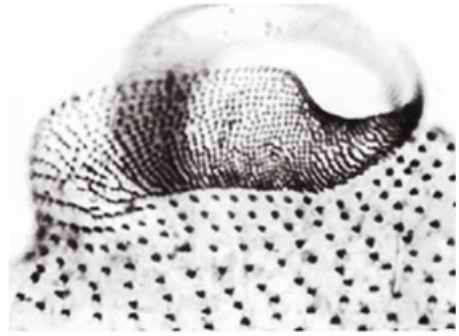

(y)

Figure 8: (a, b) *C. inflata* (Liu [77]). (c, d) *C. ecaudata* (Small and Lynn [78]). (e, f) *C. cucullus* (Small and Lynn [70]). (g, h) *C. magna* (Small and Lynn [70]). (i, j) *C. lucida* (Kim and Min [55]). (k, l) *C. aspera* (Foissner and Schubert [79]). (m, n) *C. maupasi.* (o, p) *C. henneguyi* (Kim et al. [55]). (q, r) *C. elliotti* (Foissner and Schubert [79]). (s, t) *C. spiralis* (Novotny et al. [80]). (u, v) *Colpoda steinii* (Liu [69]). (w)–(y) *C. minima* (Díaz Silvia et al. [81]).

placed in the posterior half of the body, and a comma-shaped micronucleus [30, 59, 60]. The main difference of the Chinese populations is their larger body size ($50 - 70 \times 35 - 45\,\mu$m in our populations vs. $20 - 40 \times 15 - 30\,\mu$m), which may have resulted from the increased nutrition of our cultures.

4.2. Phylogeny of Genus Colpoda. Among the polygenes with small subunit ribosomal RNA genes (SSU-rRNA), the genus *Colpoda* was nonmonophyletic, consistent with previous studies [13, 36]. Typical *Colpoda* species are unlikely to unite into a single clade because they are spread throughout the order Colpodida, and some species (e.g., *Colpoda maupasi* and *C. ecaudata*) often form unexpected clades with two or more genera that have little in common morphologically [13]. This is also observed in previously constructed phylogenies (e.g., [10, 35, 36, 56]) by Foissner et al. [61]. Dunthorn et al., [19] even proposed that there exists a strongly radiating *Colpoda*, in which several species subsequently evolved independently to form new genera and families. We augmented the taxon sampling within the genus *Colpoda* with seven newly sequenced taxa, and our results support these earlier analyses, indicating a nonmonophyletic topology of *Colpoda*. In the 18S-rRNA gene phylogenetical analysis, five *Colpoda* species (*C. reniformis*, *Colpoda* compare *grandis*, *C. inflata*, *Paracolpoda steinii*, and *C. harbinensis* n. sp.) appeared in the core of Colpodidae with medium to high support. *Paracolpoda steinii* pops. 1–4 were sister to the clade clustered by *P. steinii* and *Bromeliothrix metopoides*. This discrepancy may be due to the fact that the SSU rRNA gene is too conservative in *Colpoda* to differentiate species.

4.3. DNA Barcoding of the Colpodea Species

4.3.1. The Utility of the Cox I Gene Inaccurate Identification. Extensive barcode analyses of the animal kingdom indicate that sequence divergences in mitochondrial genes encoding *Cox I* can distinguish closely related animal species [62–64]. In the model protist genus *Tetrahymena*, intraspecific *Cox I* divergence is typically >4% [65–67]. Interestingly, *Colpoda* compare *grandis*, *C. inflata*, and *Paracolpoda steinii* differed by 12.01%–14.88% in the *Cox I* gene, strongly suggesting that the three species were distinct. In contrast, the intraspecific genetic variation of *Paracolpoda steinii* was only 0.35%, indicating that the *Cox I* gene could represent an applicable DNA barcoding region for accurate and rapid identification of *Colpoda*. However, based on our experience, we conclude that it is difficult to design primers to amplify the *Cox I* gene in *Colpoda*.

4.3.2. The Utility of the β-Tubulin Gene Inaccurate Identification. The *β-tubulin* gene is another strong candidate gene for the delineation of *Colpoda,* given that it displays a diverse array of microtubules composed of tubulin with highly similar sequences [68, 69]. Specific regions of the *β-tubulin* gene are highly conserved, making it possible to design universal primers, while regions containing hypervariable sequences can be used to generate species-specific primers for accurate identification. In this study, there were no clear boundaries between intra- and interspecific genetic distances for each of the *Colpoda*. The intraspecies variation in the *β-tubulin* gene in the *Colpoda* was considerable, as indicated by the haplotype network, with a difference of 60 genetic steps between pop. 1 and pop. 2 in *C. inflata* genetic steps (5a and 2a) (Figure 5(a)) and 69 genetic steps between pop. 3 (7) and pop. 5 (11b) in *Paracolpoda steinii* (Figure 5(b)). Therefore, the *β-tubulin* gene may be less suitable for *Colpoda* DNA barcoding than *Cox I*.

4.4. Species Identification by FISH. In this study, five probes were developed to accurately identify Colpoda (Table 3). Using *Coleps hirtus* instead of *Colpoda* species as a negative control is more effective to test the probe's specificity. Following Fried and Foissner [25], we evaluated our probes with the ARB software package and the GenBank BLAST tool to analyze the probe's specificity. Previous studies have already demonstrated the power of this method for specific delineation. Nevertheless, the probes still require consolidation with the support of isolation and/or sequencing of *Colpoda*. Our study reveals that FISH can be used for rapid and interspecific identification of *Colpoda* and can also provide some morphological information such as body shape,

macronucleus shape, and macronucleus number, which will help verify morphotypes in mixed taxa samples. However, while *Colpoda* species are geographically dispersed (e.g., Korea, U.S.A, and China), limited molecular data from disparate isolates are available [12, 13, 34, 36, 70]. The FISH probes designed here can potentially be used to investigate the geographic distribution of *Colpoda* and potentially even their dispersal.

4.5. Morphological Comparison of Colpoda harbinensis n. sp. with Other Congeners. The most important criteria for species identification in *Colpoda* are their body size and shape, oral characteristics, and the number of somatic kineties [30]. Considering the body shape, size, and number of somatic kineties, three specific species should be compared with the new species: Colpoda *inflata*, *C. maupasi*, and *C. cucullus*. Compared with *Colpoda harbinensis* n. sp. (Figure 8), *Colpoda inflata* has a different body shape (mainly "L" shaped) and more somatic kineties (20–25 vs. 11–15 in *C. harbinensis* n. sp.) [30, 57, 58]. This distinctive L-shape is produced by a marked preoral narrowing, and a hemispherical postoral portion which juts out at almost right angle vs. reniform in outline with their posterior ends broadly rounded in *C. harbinensis* n. sp. *Colpoda maupasi* is more elongated in shape ($35 - 80 \times 20 - 25\,\mu$m vs. $75 - 90 \times 50 - 66\,\mu$m in *C. harbinensis* n. sp.), with more somatic kineties (15–18 vs. 11–15 in *C. harbinensis* n. sp.) [30, 59, 71]. *Colpoda cucullus* can be easily separated from *C. harbinensis* by having more somatic kineties (26–38 vs. 11–15 in *C. harbinensis* n. sp.) and postoral kineties (8–12 vs. 3–5 in *C. harbinensis* n. sp.) [30, 58, 72].

5. Conclusion

In conclusion, our analysis is consistent with previous study showing that no single marker can delineate microbial species [73]. Combining morphological and molecular biology techniques can greatly improve the delineation of Colpodea. We suggest that *Cox I* is a promising DNA barcoding marker for species of Colpodea, as shown in this and previous studies [22, 65, 74, 75]. However, difficulties with amplification may challenge its utility in identifying this group. The FISH can provide some morphological information, thus complementing traditional techniques such as silver carbonate. Furthermore, the establishment of a character-based database may be a useful tool for resolving conflicts between morphological or molecular approaches to the differentiation of not only Colpodea but also ciliate species in general.

In conclusion, we investigated and compared the morphological features of *Colpoda reniformis*, *Colpoda* compare *grandis*, *Colpoda inflata*, and *Paracolpoda steinii*, revealed the phylogeny of Colpoda, explored the feasibilities of *Cox I* and *β-tubulin* as DNA barcoding, and supplied the identification of Colpoda species using oligonucleotide probes. In addition, we have established a new species of *Colpoda*. The novelty of this study mainly displays in following several aspects: (1) molecular techniques are used for the identification of *Colpoda* for the first time; (2) oligonucleotide probes and haplotype network analysis are firstly conducted for the identification of *Colpoda* species; and (3) the comparative exploration is made for the feasibility of *Cox I* and *β-tubulin* genes as DNA barcoding.

Data Availability

The data presented in the study are deposited in the NCBI database repository, accession numbers: OM752200, OM752201, OM752202, and OM752203.

Conflicts of Interest

The authors declare that they have no conflicts of interest.

Acknowledgments

This work was supported by the Natural Science Foundation of China (project number: 31970498) and Shenzhen Science and Technology Program (Grant No. KQTD20190929172630447). Many thanks are given to Xinyuan Zhang and Rong Gao, for their help on sampling.

References

[1] J. Y. Song, S. I. Kitamura, M. J. Oh, H. S. Kang, and S. J. Jung, "Pathogenicity of Miamiensis avidus (syn. Philasterides dicentrarchi), Pseudocohnilembus persalinus, Pseudocohnilembus hargisi and Uronema marinum (Ciliophora, Scuticociliatida)," *Diseases of Aquatic Organisms*, vol. 83, no. 2, pp. 133–143, 2009.

[2] X. Hu, X. Lin, and W. Song, *Ciliate Atlas: species found in the South China Sea*, Springer, Beijing, 2019.

[3] Y. Bai, R. Wang, W. Song, T. Suzuki, and X. Hu, "Redescription of five tintinnine ciliates (Alveolata: Ciliophora: Oligotrichea) from coastal waters of Qingdao, China," *Marine Life Science and Technology*, vol. 2, no. 3, pp. 209–221, 2020.

[4] A. McMinn, Y. Liang, and M. Wang, "Minireview: the role of viruses in marine photosynthetic biofilms," *Marine Life Science and Technology*, vol. 2, no. 3, pp. 203–208, 2020.

[5] T. Wu, Y. Li, B. Lu, Z. Shen, W. Song, and A. Warren, "Morphology, taxonomy and molecular phylogeny of three marine peritrich ciliates, including two new species: Zoothamnium apoarbuscula n. sp. and Z. apohentscheli n. sp. (protozoa, Ciliophora, Peritrichia)," *Marine Life Science and Technology*, vol. 2, no. 4, pp. 334–348, 2020.

[6] T. Zhang, J. Dong, T. Cheng, L. Duan, and C. Shao, "Reconsideration of the taxonomy of the marine ciliate Neobakuella aenigmatica moon et al., 2019 (protozoa, Ciliophora, Hypotrichia)," *Marine Life Science and Technology*, vol. 2, no. 2, pp. 97–108, 2020.

[7] W. Liu, M. K. Shin, Z. Yi, and Y. Tan, "Progress in studies on the diversity and distribution of planktonic ciliates (Protista, Ciliophora) in the South China Sea," *Marine Life Science and Technology*, vol. 3, no. 1, pp. 28–43, 2021.

[8] J. Wang, T. Zhang, F. Li, A. Warren, Y. Li, and C. Shao, "A new hypotrich ciliate, Oxytricha xianica sp. nov., with notes on the morphology and phylogeny of a Chinese population of Oxytricha auripunctata Blatterer & Foissner, 1988 (Ciliophora, Oxytrichidae)," *Marine Life Science and Technology*, vol. 3, no. 3, pp. 303–312, 2021.

[9] W. Foissner, H. Berger, and J. Schaumburg, "Identification and ecology of limnetic plankton ciliates," *Bayerisches Landesamt für Wasserwirtschaft*, vol. 3, no. 99, pp. 1–793, 1999.

[10] D. H. Lynn, A. Wright, M. Schlegel, and W. Foissner, "Phylogenetic relationships of orders within the class Colpodea (Phylum Ciliophora) inferred from small subunit rRNA gene sequences," *Journal of Molecular Evolution*, vol. 48, no. 5, pp. 605–614, 1999.

[11] M. Dunthorn and L. A. Katz, "Molecular phylogenetic analysis of class Colpodea (phylum Ciliophora) using broad taxon sampling," *Molecular Phylogenetics and Evolution*, vol. 46, no. 1, pp. 316–327, 2008.

[12] P. Quintela-Alonso, F. Nitsche, and H. Arndt, "Molecular characterization and revised systematics of Microdiaphanosoma arcuatum (Ciliophora, Colpodea)," *Journal of Eukaryotic Microbiology*, vol. 58, no. 2, pp. 114–119, 2011.

[13] W. Foissner, W. A. Bourland, K. W. Wolf, T. Stoeck, and M. Dunthorn, "New SSU-rDNA sequences for eleven colpodeans (Ciliophora, Colpodea) and description of *Apocyrtolophosis* nov. gen," *European Journal of Protistology*, vol. 50, no. 1, pp. 40–46, 2014.

[14] C. Y. Lian, Y. Y. Wang, L. F. Li, K. A. S. Al-Rasheid, J. M. Jiang, and W. B. Song, "Taxonomy and SSU rDNA-based phylogeny of three new *Euplotes* species (Protozoa, Ciliophora) from China seas," *Journal of King Saud University-Science*, vol. 32, no. 2, pp. 1286–1292, 2020.

[15] R. Wang, W. Song, Y. Bai, A. Warren, L. F. Li, and X. Z. Hu, "Morphological redescriptions and neotypification of two poorly known tintinnine ciliates (Alveolata, Ciliophora, Tintinnina), with a phylogenetic investigation based on SSU rRNA gene sequences," *International Journal of Systematic and Evolutionary Microbiology*, vol. 70, no. 4, pp. 2515–2530, 2020.

[16] S. Li, W. Zhuang, B. Pérez-Uz, Q. Q. Zhang, and X. Z. Hu, "Two anaerobic ciliates (Ciliophora, Armophorea) from China: morphology and SSU rDNA sequence, with report of a new species, Metopus paravestitus nov. spec," *Journal of Eukaryotic Microbiology*, vol. 68, article e12822, 2021.

[17] S. J. Jung, S. I. Kitamura, J. Y. Song, and M. J. Oh, "Miamiensis avidus (Ciliophora: Scuticociliatida) causes systemic infection of olive flounder Paralichthys olivaceus and is a senior synonym of Philasterides dicentrarchi," *Diseases of Aquatic Organisms*, vol. 73, no. 3, pp. 227–234, 2007.

[18] Z. Yi, W. Song, T. Stoeck et al., "Phylogenetic analyses suggest that *Psammomitra* (Ciliophora, Urostylida) should represent an urostylid family, based on small subunit rRNA and alpha-tubulin gene sequence information," *Zoological Journal of the Linnean Society*, vol. 157, no. 2, pp. 227–236, 2009.

[19] M. Dunthorn, L. A. Katz, T. Stoeck, and W. Foissner, "Congruence and indifference between two molecular markers for understanding oral evolution in the Marynidae *sensu lato* (Ciliophora, Colpodea)," *European Journal of Protistology*, vol. 48, no. 4, pp. 297–304, 2012.

[20] P. Vďačný, W. A. Bourland, W. Orsi, S. S. Epstein, and W. Foissner, "Genealogical analyses of multiple loci of litostomatean ciliates (Protista, Ciliophora, Litostomatea)," *Molecular Phylogenetics and Evolution*, vol. 65, no. 2, pp. 397–411, 2012.

[21] Z. Yi, L. Katz, and W. Song, "Assessing whether alpha-tubulin sequences are suitable for phylogenetic reconstruction of Ciliophora with insights into its evolution in euplotids," *PLoS One*, vol. 7, no. 7, article e40635, 2012.

[22] Y. Zhao, E. Gentekaki, Z. Yi, X. Lin, and Z. Li, "Genetic differentiation of the mitochondrial cytochrome oxidase c subunit I gene in genus paramecium (Protista, Ciliophora)," *PLoS One*, vol. 8, no. 10, article e77044, 2013.

[23] Y. Zhao, F. Gao, J. Q. Li, Z. Z. Yi, and A. Warren, "Phylogenetic analyses on the tintinnid ciliates (protozoa, Ciliophora) based on multigene sequence data," *Acta Protozoologica*, vol. 51, pp. 319–328, 2013.

[24] X. Chen, Y. Zhao, S. A. Al-Farraj et al., "Taxonomic descriptions of two marine ciliates, Euplotes dammamensis n. sp. and Euplotes balteatus (dujardin, 1841) Kahl, 1932 (Ciliophora, Spirotrichea, Euplotida), collected from the Arabian gulf, Saudi. Arabia," *Acta Protozoologica*, vol. 52, pp. 73–89, 2013.

[25] J. Fried and W. Foissner, "Differentiation of two very similar glaucomid ciliate morphospecies (Ciliophora, Tetrahymenida) by fluorescence in situ hybridization with 18S rRNA targeted oligonucleotide probes," *Journal of Eukaryotic Microbiology*, vol. 54, no. 4, pp. 381–387, 2007.

[26] Z. Zhan, T. Stoeck, M. Dunthorn, and K. Xu, "Identification of the pathogenic ciliate *Pseudocohnilembus persalinus* (Oligohymenophorea: Scuticociliatia) by fluorescence *in situ* hybridization," *European Journal of Protistology*, vol. 50, no. 1, pp. 16–24, 2014.

[27] Z. Zhan, J. Li, and K. Xu, "Detection and quantification of two parasitic ciliates Boveria labialis and Boveria subcylindrica (Ciliophora: Scuticociliatia) by fluorescence in situ hybridization," *Journal of Eukaryotic Microbiology*, vol. 65, no. 4, pp. 440–447, 2018.

[28] Z. Zhan and K. Xu, "Detection of two pathogenic marine ciliates Ancistrum haliotis and A. crassum (Ciliophora: Scuticociliatia) by fluorescence in situ hybridization," *Acta Oceanologica Sinica*, vol. 39, no. 12, pp. 90–94, 2020.

[29] E. B. Small and D. H. Lynn, "A new macrosystem for the phylum Ciliophora Doflein," *BioSystems*, vol. 14, no. 3-4, pp. 387–401, 1981.

[30] W. Foissner, "Colpodea (Ciliophora)," *Protozoenfauna*, vol. 4, no. 1, pp. 1–798, 1993.

[31] W. Foissner, "*Pseudomaryna australiensis* nov. gen., nov. spec. and *Colpoda brasiliensis* nov. spec., two new colpodids (Ciliophora, Colpodea) with a mineral envelope," *European Journal of Protistology*, vol. 39, no. 2, pp. 199–212, 2003.

[32] W. Foissner, "Life cycle, morphology, ontogenesis, and phylogeny of Bromeliothrix metopoides nov. gen., Nov. spec., A peculiar ciliate (Protista, Colpodea) from tank bromeliads (Bromeliaceae)," *Acta Protozoologica*, vol. 49, no. 3, pp. 159–193, 2010.

[33] M. Dunthorn, M. Eppinger, M. J. Schwarz et al., "Phylogenetic placement of the Cyrtolophosididae stokes, 1888 (Ciliophora; Colpodea) and neotypification of Aristerostoma marinum kahl, 1931," *International Journal of Systematic & Evolutionary Microbiology*, vol. 59, no. 1, pp. 167–180, 2009.

[34] W. A. Bourland, P. Vďačný, M. C. Davis, and G. Hampikian, "Morphology, morphometrics, and molecular characterization of Bryophrya gemmea n. sp. (Ciliophora, Colpodea): implications for the phylogeny and evolutionary scenario for the formation of oral ciliature in the order Colpodida," *Journal of Eukaryotic Microbiology*, vol. 58, no. 1, pp. 22–36, 2011.

[35] W. Foissner and T. Stoeck, "Morphological and molecular characterization of a new protist family, Sandmanniellidae n. fam. (Ciliophora, Colpodea), with description of Sandmanniella terricola n. g. n. sp. from the chobe floodplain in

Botswana," *Journal of Eukaryotic Microbiology*, vol. 56, pp. 472–483, 2009.

[36] P. Vďačný and W. Foissner, "Re-analysis of the 18S rRNA gene phylogeny of the ciliate class Colpodea," *European Journal of Protistology*, vol. 67, pp. 89–105, 2019.

[37] M. Liu, Y. Liu, T. Zhang et al., "Integrative studies on the taxonomy and molecular phylogeny of four new Pleuronema species (Protozoa, Ciliophora, Scuticociliatia)," *Marine Life Science and Technology*, vol. 4, pp. 179–200, 2022.

[38] M. Z. Ma, Y. Q. Li, X. Maurer-Alcala, Y. R. Wang, and Y. Yan, "Deciphering phylogenetic relationships in class Karyorelictea (Protista, Ciliophora) based on updated multi-gene information with establishment of a new order Wilbertomorphida n. ord," *Molecular Phylogenetics and Evolution*, vol. 169, article 107406, 2022.

[39] Y. Chi, X. Chen, Y. Li et al., "New contributions to the phylogeny of the ciliate class Heterotrichea (Protista, Ciliophora): analyses at family-genus level and new 618 evolutionary hypotheses," *Science China Life Sciences*, vol. 64, pp. 606–620, 2021.

[40] W. Song, D. Xu, X. Chen et al., "Overview of the diversity, phylogeny and biogeography of strombidiid oligotrich ciliates (Protista, Ciliophora), with a brief revision and a key to the known genera," *Frontiers in Microbiology*, vol. 12, article 700940, 2021.

[41] F. Gao, S. Gao, P. Wang, L. A. Katz, and W. Song, "Phylogenetic analyses of cyclidiids (Protista, Ciliophora, Scuticociliatia) based on multiple genes suggest their close relationship with thigmotrichids," *Molecular Phylogenetics and Evolution*, vol. 75, pp. 219–226, 2014.

[42] L. Jiang, C. Wang, A. Warren, H. Ma, and X. Hu, "New considerations of the systematics of the family Holophryidae (Protozoa, Ciliophora, Prostomatea) with a description of Holophrya paradiscolor sp. nov. and a redescription of Pelagothrix plancticola," *Systematics and. Biodiversity*, vol. 20, article 2012296, 2022.

[43] W. Foissner, S. Agatha, and H. Berger, "Soil ciliates (Protozoa, Ciliophora) from Namibia (Southwest Africa), with emphasis on two contrasting environments," vol. 5, pp. 1–1063, 2002, The Etosha Region and the Namib Desert.

[44] W. Foissner, "The silver carbonate methods," in *Protocols in protozoology Society of Protozoology*, pp. C7.1–C7.3, Allen Press Inc, USA, 1992.

[45] D. H. Lynn, *The Ciliated Protozoa: Characterization, Classification and Guide to the Literature*, Springer, Netherlands, 2008.

[46] T. A. Hall, "Bioedit: a user-friendly biological sequence alignment editor and analysis program for windows 95/98/nt," *Nuclc Acids Symposium Series*, vol. 41, pp. 95–98, 1999.

[47] S. Behrens, C. Ruhland, J. Inácio et al., "In situ accessibility of small-subunit rRNA of members of the domainsBacteria,Archaea, andEucaryato Cy3-labeled oligonucleotide probes," *Applied and Environmental Microbiology*, vol. 69, no. 3, pp. 1748–1758, 2003.

[48] T. Stoeck, G. T. Taylor, and S. S. Epstein, "Novel eukaryotes from the permanently anoxic Cariaco Basin (Caribbean Sea)," *Applied and Environmental Microbiology*, vol. 69, no. 9, pp. 5656–5663, 2003.

[49] A. Stamatakis, "RAxML version 8: a tool for phylogenetic analysis and post-analysis of large phylogenies," *Bioinformatics*, vol. 30, no. 9, pp. 1312-1313, 2014.

[50] F. Ronquist, M. Teslenko, P. Van Der Mark et al., "MrBayes 3.2: efficient Bayesian phylogenetic inference and model choice across a large model space," *Systematic Biology*, vol. 61, no. 3, pp. 539–542, 2012.

[51] J. A. Nylander, *MrModeltest v2. Evolutinary Biology Centre*, Uppsala University, Uppsala, Sweden, 2004.

[52] S. Kumar, G. Stecher, and K. Tamura, "MEGA7: molecular evolutionary genetics analysis version 7.0 for bigger datasets," *Molecular Biology and Evolution*, vol. 33, no. 7, pp. 1870–1874, 2016.

[53] M. D. Clement, D. Posada, and K. A. Crandall, "TCS: a computer program to estimate gene genealogies," *Molecular Ecology*, vol. 9, no. 10, pp. 1657–1659, 2000.

[54] J. W. Leigh and D. Bryant, "Popart: full-feature software for haplotype network construction," *Methods in Ecology and Evolution*, vol. 6, no. 9, pp. 1110–1116, 2015.

[55] K. S. Kim and G. S. Min, "New record of three colpodean ciliates (Ciliophora: Colpodea) from Korea," *Environmental Biology Research*, vol. 33, no. 4, pp. 375–382, 2015.

[56] J. C. Smith, "Notices of some undescribed infusoria, from the infusorial fauna of Louisiana," *Transactions of the American Microscopical Society*, vol. 19, pp. 55–68, 1897.

[57] A. C. Stokes, "Notes on some apparently undescribed infusoria from putrid waters," *The American Naturalist*, vol. 18, pp. 133–140, 1884.

[58] R. L. Burt, "Specific analysis of the genus Colpoda with special reference to the standardization of experimental material," *Transactions of the American Microscopical Society*, vol. 59, no. 4, pp. 414–432, 1940.

[59] D. H. Lynn and J. R. Malcolm, "A multivariate study of morphometric variation in species of the ciliate genusColpoda(Ciliophora: Colpodida)," *Canadian Journal of Zoology*, vol. 61, no. 2, pp. 307–316, 1983.

[60] E. Maupas, "Contribution a l'etude morphologique et anatomique des infusoires ciliés," *Archs Zool Exp Gén*, vol. 11, pp. 427–664, 1883.

[61] W. Foissner, T. Stoeck, S. Agatha, and M. Dunthorn, "Intraclass evolution and classification of the Colpodea (Ciliophora)," *Journal of Eukaryotic Microbiology*, vol. 58, no. 5, pp. 397–415, 2011.

[62] P. Hebert, A. Cywinska, S. L. Ball, and J. deWaard, "Biological identifications through DNA barcodes," *Proceedings of the Royal Society of London B*, vol. 270, no. 1512, pp. 313–321, 2003.

[63] P. Hebert, S. Ratnasingham, and J. D. Waard, "Barcoding animal life: cytochrome c oxidase subunit 1 divergences among closely related species," *Proceedings of the Royal Society of London. Series B: Biological Sciences*, vol. 270, Suppl_1, pp. S96–S99, 2003.

[64] M. Pentinsaari, P. Hebert, and M. Mutanen, "Barcoding beetles: a regional survey of 1872 species reveals high identification success and unusually deep interspecific divergences," *PLoS One*, vol. 9, no. 9, article e108651, 2014.

[65] C. Chantangsi, D. H. Lynn, M. T. Brandl, J. C. Cole, N. Hetrick, and P. Ikonomi, "Barcoding ciliates: a comprehensive study of 75 isolates of the genus Tetrahymena," *International Journal of Systematic and Evolutionary Microbiology*, vol. 57, pp. 2412–2425, 2007.

[66] F. P. Doerder, "Barcodes reveal 48 new species of Tetrahymena, Dexiostoma, and Glaucoma: phylogeny, ecology, and biogeography of new and established species," *Journal of Eukaryotic Microbiology*, vol. 66, no. 1, pp. 182–208, 2019.

[67] M. Rataj and P. Vďačný, "Multi-gene phylogeny of tetrahymena refreshed with three new histophagous species invading freshwater planarians," *Parasitology Research*, vol. 119, no. 5, pp. 1523–1545, 2020.

[68] A. B. Tourancheau, E. Villalobo, N. Tsao, A. Torres, and R. E. Pearlman, "Protein coding gene trees in ciliates: comparison with rRNA-based phylogenies," *Molecular Phylogenetics and Evolution*, vol. 10, no. 3, pp. 299–309, 1998.

[69] T. D. Edlind, G. H. Coombs, K. Vickerman, M. A. Sleigh, and A. Warren, "Phylogenetics of protozoan tubulin with reference to the amitochondriate eukaryotes," *Evolutionary Relationships Among Protozoa, Kluwer Academic Publishers, Dordrecht*, vol. 56, pp. 91–108, 1998.

[70] W. A. Bourland, G. Hampikian, and P. Vďačný, "Morphology and phylogeny of a new woodruffiid ciliate, Etoschophrya inornata sp. n. (Ciliophora, Colpodea, Platyophryida), with an account on evolution of platyophryids," *Zoologica Scripta*, vol. 41, no. 4, pp. 400–416, 2012.

[71] P. Enrioues, "Sulla morfologia e sistematica del genere Colpoda," *Archives de Zoologie Expérimentale et Générale*, vol. 8, pp. 1–15, 1908.

[72] O. F. Müller, "Animalcula Infusoria Fluviatilia et Marina, quae Detexit, Systematice Descripsit et ad Vivum Delineari Curavit N Mölleri Hauniae," 1786.

[73] J. Pawlowski, S. Audic, S. Adl et al., "CBOL protist working group: barcoding eukaryotic richness beyond the animal, plant, and fungal kingdoms," *PLoS Biology*, vol. 10, no. 11, article e1001419, 2012.

[74] C. P. Kher, F. P. Doerder, J. Cooper et al., "Barcoding *Tetrahymena*: discriminating species and identifying unknowns using the cytochrome _c_ oxidase subunit I (cox-1) barcode," *Protist*, vol. 162, no. 1, pp. 2–13, 2011.

[75] S. Tarcz, M. Rautian, A. Potekhin et al., "*Paramecium putrinum* (Ciliophora, Protozoa): the first insight into the variation of two DNA fragments - molecular support for the existence of cryptic species," *Molecular Phylogenetics and Evolution*, vol. 73, pp. 140–145, 2014.

[76] I. Whang, H. S. Kang, and J. Lee, "Identification of scuticociliates (Pseudocohnilembus persalinus P. longisetus Uronema marinum and Miamiensis avidus) based on the cox1 sequence," *Parasitology International*, vol. 62, no. 1, pp. 7–13, 2013.

[77] H. C. Liu, *Studies on Classification and Species Diversity of Ciliates in Plateau Swamp Wetlands in Gannan, Gansu in Spring*, Northwest Normal University, China, 2010.

[78] E. B. Small and D. H. Lynn, "A new macrosystem for the phylum ciliophora doflein, 1901," *Bio Systems*, vol. 14, no. 3-4, pp. 387–401, 1981.

[79] W. Foissner and G. Schubert, "Morphologische und diskriminanzanalytische trennung von colpoda aspera kahl, 1926 und colpoda elliotti bradbury et outka, 1967 (ciliophora: colpodidae)," *Acta Protozoologica*, vol. 22, pp. 127–138, 1983.

[80] R. T. Novotny, D. H. Lynn, and F. R. Evans, "Colpoda spiralis sp. n., a Colpodid ciliate found inhabiting treeholes (Colpodida, Ciliophora)," *Journal of Protozoology*, vol. 24, no. 3, pp. 364–369, 1977.

[81] D. Silvia, D. Martín-González Ana, G. Rico, and J. Carlos, "Morphogenesis of the division and encystment process of the ciliated protozoanColpoda minima," *Journal of Natural History*, vol. 37, no. 20, pp. 2395–2412, 2003.